

# Hybrid [5]Radialenes with Bispyrroloheteroles: New Electron-Donating Units

Tomohiro Higashino,<sup>[a]</sup> and Hiroshi Imahori<sup>\*[a,b]</sup>

**Abstract:** Bispyrroloheteroles have been synthesized to address their intrinsic structural, optical and electrochemical properties. The X-ray crystal structures and calculated natural bond orbital (NBO) bond orders unambiguously demonstrated the existence of a two pyrrole-fused five-membered ring with short exocyclic C=C double bonds and long endocyclic C–C single bonds, supporting that the bispyrroloheteroles are the rare examples of structurally characterized hybrid [5]radialenes. The bispyrroloheteroles were found to act as an electron-donating unit, which would be fascinating for the rational design of novel charge-transporting and donor/acceptor photovoltaic materials as well as versatile charge-transfer complexes.

## Introduction

Radialenes are cross-conjugated cyclic molecules in which all carbon atoms are  $sp^2$ -hybridized in the ring and there are, as much as possible, exocyclic C=C double bonds.<sup>[1]</sup> After the first synthesis of [6]radialene by Hopff and Wick in 1961,<sup>[2]</sup> various radialenes and their derivatives have intensively been explored from both experimental and theoretical viewpoints because of their unique reactivity and electronic properties.<sup>[1,3–5]</sup> Since new synthetic approaches make radialenes more accessible, electron-rich or electron-deficient radialenes have been used as novel  $\pi$ -donors and  $\pi$ -acceptors for the charge-transfer (CT) complexes, respectively.<sup>[6]</sup>

In recent years, radialenes with fused aromatic rings are also of interest due to their possible aromaticity and electronic structures.<sup>[6a,d,7]</sup> Triphenylene **1** and dibenzothiophene **2** are not basically considered as radialenes owing to the extended delocalization of the  $\pi$ -electrons in the aromatic sextet (Figure 1).<sup>[1]</sup> On the other hand, the thiophene-fused compound **3**, which is isoelectronic with triphenylene, may certainly be regarded as a [6]radialene by X-ray structural analysis.<sup>[7a]</sup> In this regard, the use of heterole-fused ring system could be an effective means of creating novel radialene derivatives.<sup>[7b]</sup>

In contrast to the rapid development of conventional

[ $n$ ]radialenes, hybrid [ $n$ ]radialenes possessing a heteroatom in the ring are still limited despite of their attractive electronic properties.<sup>[1b,8–10]</sup> Yoshifuji,<sup>[8a]</sup> Brieden,<sup>[8b]</sup> Majoral<sup>[8c]</sup> and Lammertsma<sup>[8d]</sup> *et al.* reported phospho-hybrid radialenes, which were characterized by X-ray structural analysis. Radialene derivatives of heterole analogues, hybrid [5]radialenes, are rather elusive.<sup>[9]</sup> Trahanovsky and co-workers described the generation of furanoradialene (oxa-hybrid [5]radialene) by the flash vacuum pyrolysis (FVP).<sup>[9a]</sup> Other hybrid [5]radialenes have been synthesized by using heterole-fused ring system, such as dithienothiophene **4** (Figure 1).<sup>[9b,e]</sup> However, to the best of our knowledge, there is no structural analysis and systematic evaluation of their basic properties. Herein, we report a systematic series of bispyrroloheteroles as the rare examples of structurally characterized hybrid [5]radialenes. The X-ray crystal analysis and theoretical calculations have been conducted to assess their nature as hybrid [5]radialenes. The optical and electrochemical properties have also been examined by UV/vis absorption and fluorescence spectra and cyclic voltammetry (CV) and differential pulse voltammetry (DPV) measurements.

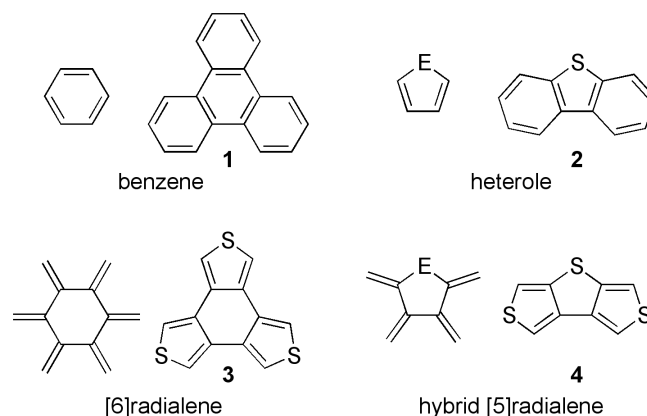


Figure 1. Representative examples of (hetero)arenes and radialenes.

## Results and Discussion

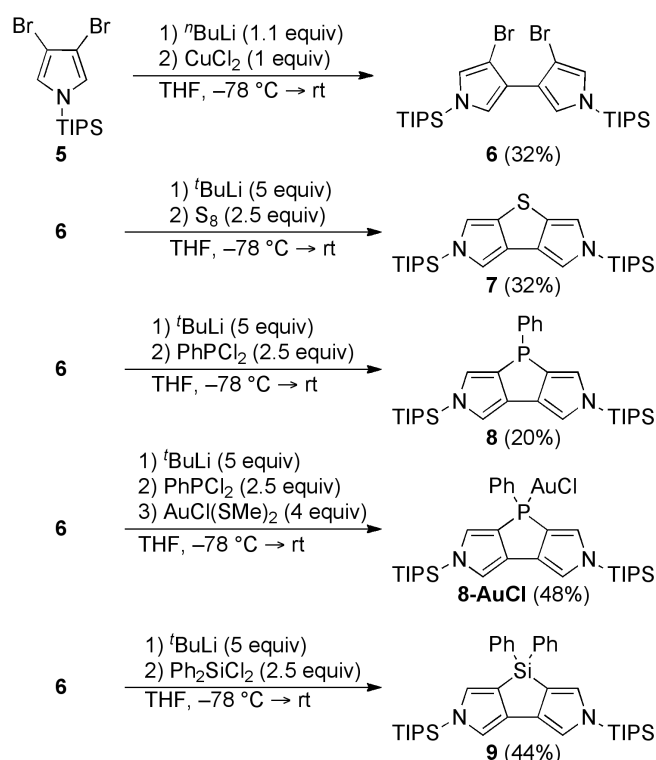
Bispyrroloheteroles were synthesized by the route shown in Scheme 1. 4,4'-Dibromo-3,3'-bipyrrole **6** was prepared by dimerization of 3,4-dibromopyrrole **5**<sup>[11]</sup> in moderate yield (32%) as a key intermediate. Then, we attempted double halogen-lithium exchange of **6**. The treatment with almost stoichiometric amount of <sup>t</sup>BuLi smoothly generated dilithium species of **6**, while a large excess amount (>10 equiv) of <sup>n</sup>BuLi was necessary for the corresponding reaction. This result encouraged us to start the synthesis of bispyrroloheteroles. Treatment of **6** with <sup>t</sup>BuLi followed by the addition of elemental sulfur provided

[a] Dr. T. Higashino, Prof. Dr. H. Imahori  
Department of Molecular Engineering, Graduate School of  
Engineering  
Kyoto University  
Nishikyo-ku, Kyoto, 615-8510, Japan  
E-mail: imahori@scl.kyoto-u.ac.jp

[b] Prof. Dr. H. Imahori  
Institute for Cell-Material Sciences (WPI-iCeMS)  
Kyoto University  
Nishikyo-ku, Kyoto, 615-8510, Japan

Supporting information for this article is given via a link at the end of the document.

bispyrrolothiophene **7** in 32% yield. Bispyrrolophosphole **8** and bispyrrolosilole **9** were prepared in 20% and 44% yield by similar manner with dichlorophenylphosphine and dichlorodiphenylsilane as the electrophiles, respectively. It is noteworthy that phosphole **8** is the first example of phosphahybrid [5]radialene derivative. Phosphole **8** was found to be rather unstable under ambient atmosphere. To stabilize the structure, crude **8** was further converted into the gold(I) complex **8-AuCl** (48% based on **6**). Unfortunately, demetalation of **8-AuCl** with  $P(NMe_2)_3$  did not give phosphole **8**, probably due to the high coordination ability derived from its electron-rich nature. All the new compounds were characterized by  $^1H$  and  $^{13}C$  NMR, high-resolution MS, and FT-IR spectroscopies (Figures S1-S7).



**Scheme 1.** Synthesis of 4,4'-dibromo-3,3'-bipyrrrole **6** and bispyrroloheteroles **7-9**.

Single crystals suitable for X-ray diffraction analysis (Table S1) were also obtained for **7**, **8-AuCl**, **9**, and **10** (vide infra).<sup>[12a-c]</sup> These crystal structures unambiguously revealed that bispyrroloheteroles have a planer tricyclic structure (Figures 2a-c). In the crystal packing, there are  $CH \cdots \pi$  interactions between the TIPS moiety and the bispyrroloheterole plane in **7**, **8-AuCl**, and **10**, whereas that between the phenyl group and the bispyrroloheterole plane is evident in **9**. Thus, such intermolecular  $CH \cdots \pi$  interactions prevail between the molecules (Figures S8a-c). The selected bond lengths of these bispyrroloheteroles are summarized in Table 1. The pyrrolic  $C_\alpha-C_\beta$  bond lengths ( $a/a'$  and  $b/b'$  in Table 1) of **7**, **8-AuCl**, and **9** are in the range of 1.363–1.372 Å, which are almost comparable to

a typical C=C bond length (1.35 Å) in 1,3-butadiene.<sup>[13]</sup> In contrast, the C–C bond lengths in heterole moiety ( $d/d'$  and  $e$  in Table 1) are within 1.425–1.467 Å, which are quite similar to a C–C single bond length in 1,3-butadiene (1.47 Å).<sup>[13]</sup> Taking into account that the typical C–C bond length in benzene is 1.40 Å,<sup>[14]</sup> the pyrrolic  $C_\alpha-C_\beta$  bonds and the C–C bonds in the heterole moiety can be regarded as C=C double bonds and C–C single bonds, respectively. These characteristic structural features, short exocyclic C=C bonds and long endocyclic C–C bonds, clearly support that these bispyrroloheteroles are a family of hybrid [5]radialenes.

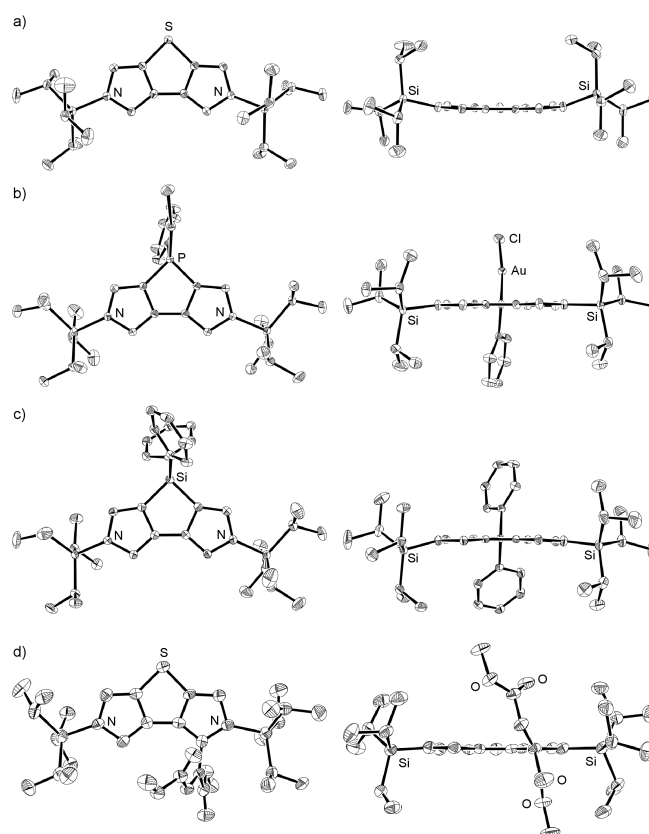


**Figure 2.** X-Ray crystal structures of a) **7**, b) **8-AuCl**, c) **9**, and d) **10**: top view (left) and side view (right). For **8-AuCl**, one of the two independent molecules in the unsymmetric unit cell is shown. Thermal ellipsoids represent 50% probability. Solvent molecules and hydrogen atoms are omitted for clarity.

**Table 1.** Selected bond lengths in crystal structures.

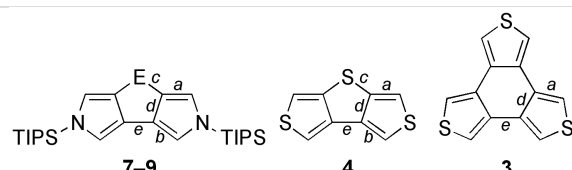
bond length / Å	<b>7</b>	<b>8-AuCl</b> <sup>[a]</sup>	<b>9</b>
$a$	1.3698(18)	1.370(4)	1.3659(17)

<i>a'</i>	1.3710(18)	1.369(4)	1.3695(18)
<i>b</i>	1.3719(18)	1.363(4)	1.3643(18)
<i>b'</i>	1.3679(19)	1.367(4)	1.3692(18)
<i>c</i>	1.7682(14)	1.804(3)	1.8627(13)
<i>c'</i>	1.7662(13)	1.793(3)	1.8604(13)
<i>d</i>	1.4248(19)	1.431(4)	1.4490(18)
<i>d'</i>	1.4292(18)	1.440(4)	1.4451(18)
<i>e</i>	1.4488(18)	1.457(4)	1.4674(17)

[a] Data of one of the two independent molecules in the unsymmetric unit cell.

Natural bond orbital (NBO) bond orders provide a measure of the order of a bond from a calculated wave function.<sup>[15]</sup> To further ensure the radialene structures, we calculated the NBO bond orders of **7–9** as well as of thia-hybrid [5]radialene **4** and [6]radialene **3** as references (Table 2). The NBO bond orders of the exocyclic C–C bonds of **7–9** (*a* and *b* in Table 2) range from 1.484 to 1.560. These values largely agree with those of thia-hybrid [5]radialene **4** (*a* and *b* in Table 2, 1.589 and 1.544) and [6]radialene **3** (*a* in Table 2, 1.555). Thus, these C–C bonds can be assigned to C=C double bonds. Meanwhile, the NBO bond orders of endocyclic C–C bonds of **7–9** (*d* and *e* in Table 2) are in the range of 1.064–1.220. Considering the NBO bond orders of endocyclic C–C bonds of **4** (*d* and *e* in Table 2, 1.178 and 1.072) and **3** (*d* and *e* in Table 2, 1.176 and 1.066), these endocyclic C–C bonds can be identified as single bonds. These NBO bond orders are consistent with the hybrid [5]radialene structures of the bispyrroloheteroles, which were determined by the X-ray crystal analysis.

Table 2. NBO bond orders.<sup>[a]</sup>

NBO bond order					
	<b>7</b>	<b>8</b>	<b>9</b>	<b>4</b>	<b>3</b>
<i>a</i>	1.527	1.554	1.526	1.589	1.555
<i>b</i>	1.484	1.511	1.560	1.544	
<i>c</i>	1.062	0.917	0.744	1.056	
<i>d</i>	1.213	1.218	1.220	1.178	1.176
<i>e</i>	1.091	1.074	1.064	1.072	1.066

[a] Calculated on the optimized structures at B3LYP/6-31G(d,p) level.

The hybrid [5]radialene-type structures of **7–9** are also supported by computed NICS(0) values at B3LYP/6-31G(d,p) level (Figure 3).<sup>[16]</sup> The NICS(0) values of **7** (–5.61 ppm) and **8** (+0.06 ppm) are considerably less negative than those of thiophene (–13.64 ppm) and phosphole (–4.99 ppm) that possess 6 $\pi$ -aromatic character. It is noteworthy that the NICS(0) value of **9** is comparable to non-aromatic silole, indicating that the pyrrole ring has almost no deshielding effect on central heterole ring. Therefore, the less negative NICS(0) values of **7** and **8** can be explained by loss of 6 $\pi$ -aromatic character because of the hybrid [5]radialene-type structure, not by the local diamagnetic ring current effect of the pyrrole rings.

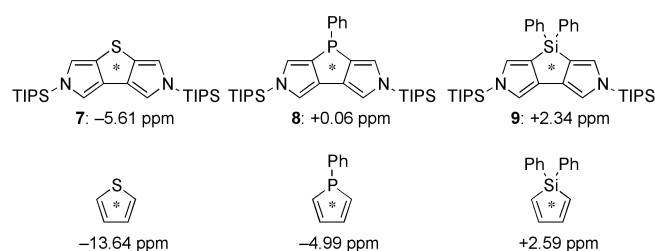
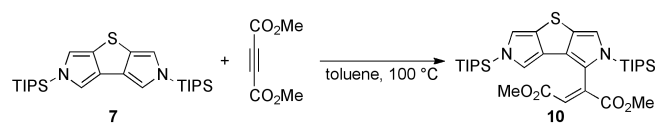


Figure 3. GIAO-SCF calculated NICS(0) values at the gravity centers of central rings.

Then, we examined the reaction of **7** with dimethyl acetylenedicarboxylate (DMAD) as a typical example to obtain insight into the reactivities of bispyrroloheteroles. Sha and co-workers reported the Diels-Alder reaction of *N*-benzyl analogue of **7** with DMAD.<sup>[9d]</sup> Contrary to this, heating a solution of **7** and DMAD in toluene gave Michael-type adduct **10** in 32% yield (Scheme 2). In general, the reaction of pyrroles and DMAD affords two kinds of products, Diels-Alder and Michael-type adducts.<sup>[17]</sup> Pyrroles with bulky substituents such as *t*-butyl group on the nitrogen atom are reacted with DMAD, to give 1:1 Michael-type adducts at the 2-position, whereas the reaction of less sterically hindered pyrroles, such as *N*-benzylpyrrole, with DMAD forms Diels-Alder adducts. In the present case, the reaction of **7** with DMAD furnished the Michael-type adduct **10** as a sole product probably due to the larger congestion of the TIPS moieties than the *t*-butyl ones. Finally, the structure of **10** was unambiguously confirmed by single crystal X-ray diffraction analysis (Figure 2d).<sup>[12d]</sup> It should be pointed out that the short contact of sulfur atoms (3.48 Å) in the packing structure indicates the intermolecular S–S interaction in the solid state (Figure S8d).



Scheme 2. Reaction of **7** with DMAD yielding Michael-type adduct **10**.

We measured UV/vis absorption and fluorescence spectra of **7–10** in cyclohexane (Figure 4). The absorption spectra of bispyrroloheteroles **7–9** are almost identical and exhibit  $\pi\text{-}\pi^*$  transitions at around 260 nm. In the case of thiophene derivative **7**, weak absorption is observed at around 300 nm, which probably reflects the contribution of  $n\text{-}\pi^*$  transition of the thiophene ring. The fluorescence spectra of **7–9** display broad emissions in the blue region (300–400 nm). The fluorescence maxima of phosphole **8** (370 nm) and silole **9** (362 nm) are red-shifted relative to that of thiophene **7** (316 nm). In addition, **8** and **9** show comparable fluorescence intensities, which are larger than **7**. Note that the wavelength of the emission maxima is independent on excitation wavelength. Therefore, the heteroatoms in **7–9** mainly affect the character of the excited states rather than the ground state. The absorption spectrum of **8-AuCl** is almost the same as that of **8**, while the fluorescence is intensively quenched by gold(I) ion (Figure S9). The absorption spectrum of **10** is similar to that of **7** in the UV region ( $< 320$  nm). It is notable that a broad and weak absorption is observed for **10** at around 440 nm, which can be attributed to intramolecular charge-transfer (ICT) interaction between the electron-donating bispyrrolothiophene and electron-withdrawing ethylenedicarboxylate. We measured the absorption spectra of **10** in various solvents and found that **10** reveals solvatochromism (Figure S10). In addition, the fluorescence spectrum of **10** shows a broad CT emission at around 510 nm (Figure S11).

255 nm were adjusted to be identical (0.1) and the samples were excited at 255 nm under the same excitation condition for accurate intensity comparison.

The electrochemical properties were studied by CV and DPV in  $\text{CH}_2\text{Cl}_2$  versus ferrocene/ferrocenium ion ( $\text{Fc}/\text{Fc}^+$ ) with tetra-*n*-butylammonium hexafluorophosphate as an electrolyte (Figure 5). While no reduction peak appears for **7–9** at potentials up to  $-2.5$  V, the bispyrroloheteroles exhibit oxidation peaks at 0.29 V for **7**, 0.30 V for **8**, and 0.31 V for **9**. These oxidation potentials are similar to those of electron-donating radicalene derivatives that can form CT complexes.<sup>[6a–d]</sup> Given that the energy level of  $\text{Fc}/\text{Fc}^+$  is  $-4.8$  eV under vacuum,<sup>[18]</sup> the HOMO energy levels of **7–9** should be located at ca.  $-5.1$  eV under vacuum. The HOMO levels of **7–9** are in the middle of those of TTF ( $-4.78$  eV) and perylene ( $-5.3$  eV),<sup>[19]</sup> which are typical donor molecules for conducting CT complexes.<sup>[20]</sup> Furthermore, the HOMO levels of the electron-donating building blocks for donor-acceptor copolymers, such as benzodithiophenes and dithioenosiols (ca.  $-5.5$  eV), are lower than those of **7–9**.<sup>[21]</sup> By contrast, **10** displays a reversible reduction peak at  $-1.97$  V as well as a reversible oxidation peak at 0.38 V as the result of introduction of the electron-accepting ethylenedicarboxylate moiety into the electron-donating bispyrrolothiophene. The low oxidation potentials of **7–10** reflect their electron-rich nature, which would make it possible to utilize the bispyrroloheteroles as novel  $\pi$ -donors for charge-transporting and donor/acceptor photovoltaic materials as well as CT complexes.

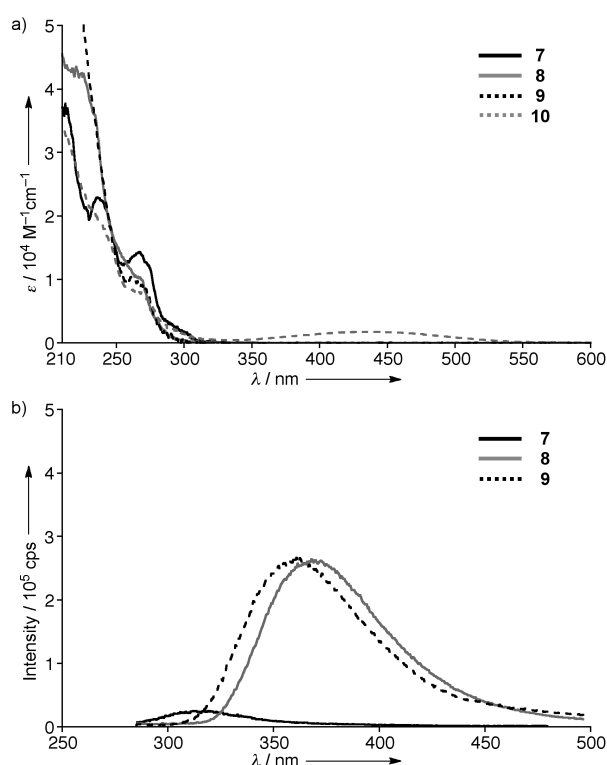


**Figure 4.** a) UV/vis absorption spectra of **7–10** and b) fluorescence spectra of **7–9** in cyclohexane. For the fluorescence measurements, the absorbances at

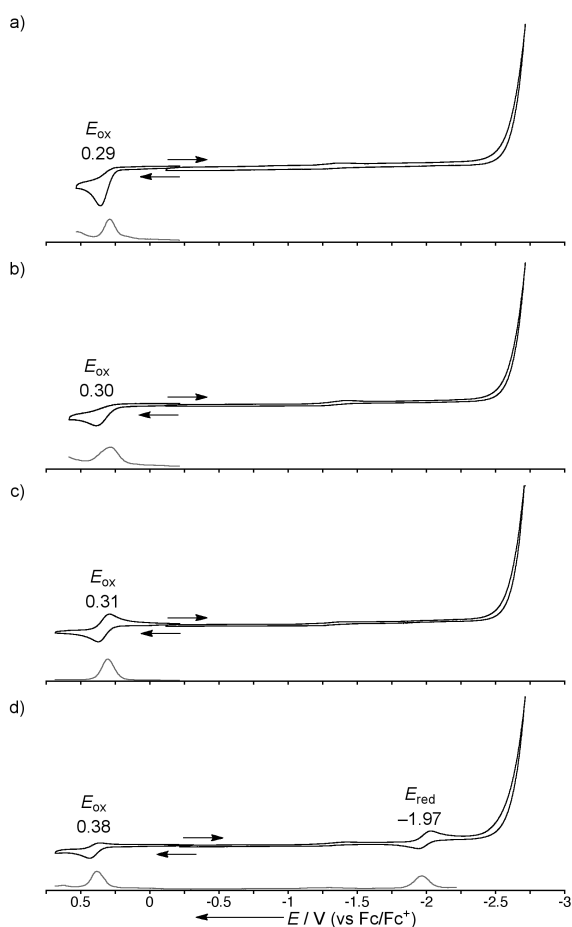


**Figure 5.** Cyclic voltammograms (black) and DPV curves (gray) of a) **7**, b) **8**, c) **9**, and d) **10**. Redox potentials were determined by DPV. Solvent:  $\text{CH}_2\text{Cl}_2$ ; scan rate:  $0.05 \text{ V s}^{-1}$ ; working electrode: glassy carbon; reference electrode:  $\text{Ag}/\text{Ag}^+$  ( $0.01 \text{ M AgNO}_3$ ); electrolyte:  $\text{Bu}_4\text{NPF}_6$ .

To gain the further insight into the electronic structures of the bispyrroloheteroles, we performed DFT calculations at B3LYP/6-31G(d,p) level. The selected molecular orbitals of **7–10** are illustrated in Figure S12. The HOMO of **7** has a large electron density on the sulfur atom, indicating largely thiophene-based electronic structure. The LUMO of **7** is delocalized on the bipyrrole skeleton, in which the sulfur atom has no electron density. Consequently, the sulfur atom mainly has an impact on the HOMO of **7**. Since the phosphorus and silicon atoms in **8** and **9** are on the node of the HOMOs, the heteroatoms make little contribution to the electronic structure of the HOMOs. In contrast, the LUMOs of **8** and **9** possess large electron densities on the phenylphosphinic and diphenylsilyl moieties. The electronic structures of **8** and **9** resemble those of typical phospholes and siloles.<sup>[22]</sup> The time-dependent DFT (TD-DFT) calculations qualitatively reproduce the absorption features of bispyrroloheteroles **7–10** (Table S2). The  $\pi\text{--}\pi^*$  transitions of **7–9** exhibit large oscillator strengths ( $f > 0.2$ ) and comparable excitation energies (ca. 243 nm). The HOMO–LUMO transition

of **7** displays the higher oscillator strength ( $f = 0.0085$ ) than those of **8** and **9** ( $f = 0.0004$  and  $0.0018$ ), which is in good agreement with the weak absorption of **7** at around 300 nm in cyclohexane. The HOMO and LUMO of **10** are localized on the bispyrrolothiophene and ethylenedicarboxylate moieties, respectively, which rationalizes the appearance of the ICT band of **10** in the nonpolar solvent.

## Conclusions

In summary, we have successfully synthesized a systematic series of the bispyrroloheteroles via key intermediate dibromobipyrrole **6** to elucidate their intrinsic structural, optical and electrochemical properties. The X-ray structural analysis and calculated NBO bond orders unambiguously demonstrated the existence of the three fused five-membered rings with short exocyclic C=C double bonds and long endocyclic C–C single bonds. Therefore, the bispyrroloheteroles **7–9** are the rare examples of structurally characterized hybrid [5]radialenes. It should be emphasized that the phosphole derivative is the first example of phospho-hybrid [5]radialenes. The electron-donating bispyrroloheteroles **7–9** are highly promising as novel  $\pi$ -donors for yielding CT interactions in the corresponding donor/acceptor complexes. Indeed, the Michael-type adduct **10** obtained from the reaction of **7** with DMAD displayed a distinct ICT absorption. Bispyrroloheteroles are a new class of radialenes, which will be very useful as electron-donating building blocks for charge-transporting and donor/acceptor photovoltaic materials.

## Experimental Section

**Instrumentation and Materials:** Commercially available solvents and reagents were used without further purification unless otherwise mentioned. Silica-gel column chromatography was performed with UltraPure Silica Gel (230–400 mesh, SiliCycle) unless otherwise noted. Thin-layer chromatography (TLC) was performed with Silica gel 60 F<sub>254</sub> (Merck). UV/vis/NIR absorption spectra were measured with a Perkin-Elmer Lambda 900 UV/vis/NIR spectrometer. Steady-state fluorescence spectra were obtained by a HORIBA Nanolog spectrometer.  $^1\text{H}$  and  $^{13}\text{C}$  NMR spectra were recorded with a JEOL ECX-400P spectrometer (operating at 395.88 MHz for  $^1\text{H}$  and 99.54 MHz for  $^{13}\text{C}$ ) by using the residual solvent as the internal reference for  $^1\text{H}$  ( $\text{CDCl}_3$ :  $\delta = 7.26 \text{ ppm}$ ) and  $^{13}\text{C}$  ( $\text{CDCl}_3$ :  $\delta = 77.16 \text{ ppm}$ ).  $^{31}\text{P}$  NMR spectrum was recorded with a JEOL EX-400 spectrometer (operating at 161.7 MHz for  $^{31}\text{P}$ ) by using trimethylphosphite as the external reference for  $^{31}\text{P}$  ( $\delta = 140 \text{ ppm}$ ). High-resolution mass spectra (HRMS) were measured on a Thermo Fischer Scientific EXACTIVE spectrometer. Attenuated total reflectance-Fourier transform infrared (ATR-FTIR) spectra were taken with the golden gate diamond anvil ATR accessory (NICOLET 6700, Thermo scientific), using typically 64 scans at a resolution of  $2 \text{ cm}^{-1}$ . All samples were placed in contact with the diamond window using the same mechanical force. Single-crystal X-ray diffraction analysis data for compounds **7**, **8-AuCl**, **9**, and **10** were collected at  $-150 \text{ }^\circ\text{C}$  on a Rigaku Saturn70 CCD diffractometer with graphite monochromated  $\text{Mo-K}_\alpha$  radiation ( $0.71069 \text{ \AA}$ ). The structures were solved by direct method (SHELXS-2013). Redox potentials were measured by cyclic voltammetry and differential pulse voltammetry method on an ALS electrochemical analyzer model 660A.

**Synthesis:** 3,4-Dibromo-1-triisopropylsilylpyrrole (**5**) was prepared according to literature.<sup>[11]</sup>

#### 4,4'-Dibromo-1,1'-bis(triisopropylsilyl)-3,3'-bipyrrrole (**6**):

A 1.55 M solution of <sup>n</sup>BuLi in <sup>n</sup>hexane (3.6 mL, 5.5 mmol) was added dropwise to a solution of dibromopyrrole **5** (1.90 g, 5.0 mmol) in anhydrous THF (50 mL) at -78 °C under Ar atmosphere. After the solution was stirred for 15 min, anhydrous CuCl<sub>2</sub> (672 mg, 5.0 mmol) was added by one portion. The mixture was stirred for 15 min and then warmed to room temperature. After the mixture was stirred for 60 min, the reaction was quenched with saturated NH<sub>4</sub>Cl aq (50 mL) and the product was extracted with CH<sub>2</sub>Cl<sub>2</sub> (50 mL ×3). The combined organic layer was washed with water and brine, and dried over Na<sub>2</sub>SO<sub>4</sub>. After the solvent was removed, the crude product was purified by silica gel chromatography using a 1:15 mixture of CH<sub>2</sub>Cl<sub>2</sub> and <sup>n</sup>hexane to give **6** as a colorless solid (488 mg, 0.81 mmol, 32%). <sup>1</sup>H NMR (395.88 MHz, CDCl<sub>3</sub>, 25 °C): δ = 7.20 (d, *J* = 2.3 Hz, 2H, α-H), 6.78 (d, *J* = 2.3 Hz, 2H, α-H), 1.45 (septet, *J* = 7.7 Hz, 6H, -SiCH(CH<sub>3</sub>)<sub>2</sub>) and 1.12 (d, *J* = 7.7 Hz, 36H, -SiCH(CH<sub>3</sub>)<sub>2</sub>) ppm; <sup>13</sup>C NMR (99.54 MHz, CDCl<sub>3</sub>, 25 °C): δ = 123.8, 122.9, 118.0, 98.7, 17.9 and 11.7 ppm. FT-IR (ATR): ν = 2944, 2890, 2866, 1482, 1462, 1366, 1251, 1206, 1090, 1015, 993, 970, 920, 903, 883, 779, 694, 659, 578 and 527 cm<sup>-1</sup>. HRMS (APCI, positive) calcd. for C<sub>26</sub>H<sub>47</sub>Br<sub>2</sub>N<sub>2</sub>Si<sub>2</sub> [M+H]<sup>+</sup> 601.1639; found 601.1630. m.p.: 126–128 °C.

#### 2,6-Bis(triisopropylsilyl)-thieno[2,3-c:4,5-c']dipyrrrole (**7**):

A 1.6 M solution of <sup>t</sup>BuLi in <sup>n</sup>pentane (0.16 mL, 250 μmol) was added dropwise to a solution of dibromobipyrrrole **6** (30 mg, 50 μmol) in anhydrous THF (5 mL) at -78 °C under Ar atmosphere. The mixture was stirred for 10 min and then stirred for 15 min at room temperature. After recoiling to -78 °C, S powder (4.0 mg, 125 μmol) was added by one portion. The mixture was stirred for 10 min and then warmed to room temperature. After the mixture was stirred for 60 min, the reaction was quenched with water (5 mL) and the product was extracted with CH<sub>2</sub>Cl<sub>2</sub> (10 mL ×3). The combined organic layer was washed with water and brine, and dried over Na<sub>2</sub>SO<sub>4</sub>. After the solvent was removed, the crude product was purified by silica gel chromatography using a 1:9 mixture of CH<sub>2</sub>Cl<sub>2</sub> and <sup>n</sup>hexane to give **7** as a colorless solid (7.7 mg, 16 μmol, 32%). Single crystals suitable for X-ray crystallographic analysis were obtained by vapor diffusion of <sup>n</sup>hexane into a solution of **7** in CH<sub>2</sub>Cl<sub>2</sub>. <sup>1</sup>H NMR (395.88 MHz, CDCl<sub>3</sub>, 25 °C): δ = 6.92 (d, *J* = 1.8 Hz, 2H, α-H), 6.67 (d, *J* = 1.8 Hz, 2H, α-H), 1.47 (septet, *J* = 7.8 Hz, 6H, -SiCH(CH<sub>3</sub>)<sub>2</sub>) and 1.12 (d, *J* = 7.8 Hz, 36H, -SiCH(CH<sub>3</sub>)<sub>2</sub>) ppm; <sup>13</sup>C NMR (99.54 MHz, CDCl<sub>3</sub>, 25 °C): δ = 130.4, 123.5, 113.7, 112.9, 18.0 and 11.9 ppm. UV/vis (cyclohexane): λ (ε, M<sup>-1</sup> cm<sup>-1</sup>) = 238 (23000), 265 (13000) and 300(sh) (1000) nm. Fluorescence (cyclohexane, λ<sub>ex</sub> = 255 nm): λ<sub>max</sub> = 316 nm. FT-IR (ATR): ν = 2944, 2888, 2865, 1467, 1359, 1259, 1213, 1198, 1067, 1016, 992, 959, 883, 754, 693, 674, 660, 636, 615, 596, 561 and 524 cm<sup>-1</sup>. HRMS (APCI, positive) calcd. for C<sub>26</sub>H<sub>47</sub>N<sub>2</sub>SSi<sub>2</sub> [M+H]<sup>+</sup> 475.2993; found 475.2988. m.p.: 137–139 °C.

#### 2,6-Bis(triisopropylsilyl)-4-phenylphospholo[2,3-c:4,5-c']dipyrrrole (**8**):

A 1.6 M solution of <sup>t</sup>BuLi in <sup>n</sup>pentane (0.16 mL, 250 μmol) was added dropwise to a solution of dibromobipyrrrole **6** (30 mg, 50 μmol) in anhydrous THF (5 mL) at -78 °C under Ar atmosphere. The mixture was stirred for 10 min and then stirred for 15 min at room temperature. After recoiling to -78 °C, PhPCl<sub>2</sub> (17 μL, 125 μmol) was added by one portion. The mixture was stirred for 10 min and then warmed to room temperature. After the mixture was stirred for 60 min, the reaction was quenched with water (5 mL) and the product was extracted with CH<sub>2</sub>Cl<sub>2</sub> (10 mL ×3). The combined organic layer was washed with water and brine, and dried over

Na<sub>2</sub>SO<sub>4</sub>. After the solvent was removed, the crude product was purified by silica gel chromatography using a 1:4 mixture of CH<sub>2</sub>Cl<sub>2</sub> and <sup>n</sup>hexane to give **8** as a colorless solid (5.6 mg, 10 μmol, 20%). <sup>1</sup>H NMR (395.88 MHz, CDCl<sub>3</sub>, 25 °C): δ = 7.45 (t, *J* = 7.3 Hz, 2H, *meta*-H), 7.20 (m, 2H, *ortho*-H), 7.17 (m, 1H, *para*-H), 6.87 (d, *J* = 1.2 Hz, 2H, α-H), 6.81 (d, *J* = 1.2 Hz, 2H, α-H), 1.45 (septet, *J* = 7.8 Hz, 6H, -SiCH(CH<sub>3</sub>)<sub>2</sub>) and 1.11 (dd, *J* = 7.8 Hz, *J* = 6.3 Hz, 36H, -SiCH(CH<sub>3</sub>)<sub>2</sub>) ppm; <sup>13</sup>C NMR (99.54 MHz, CDCl<sub>3</sub>, 25 °C): δ = 130.9, 130.8 (d, *J* = 19 Hz), 128.8, 128.1 (m), 127.5, 124.5, 124.3, 114.0 (m), 18.0 and 11.9 ppm; <sup>31</sup>P NMR (161.7 MHz, CDCl<sub>3</sub>, 25 °C): δ = -42.46 ppm. UV/vis (cyclohexane): λ (ε, M<sup>-1</sup> cm<sup>-1</sup>) = 268 (10000) nm. Fluorescence (cyclohexane, λ<sub>ex</sub> = 255 nm): λ<sub>max</sub> = 370 nm. FT-IR (ATR): ν = 2943, 2889, 2865, 2359, 1468, 1356, 1221, 1189, 1089, 1069, 1014, 994, 918, 883, 779, 692, 662, 589 and 522 cm<sup>-1</sup>. HRMS (APCI, positive) calcd. for C<sub>32</sub>H<sub>52</sub>N<sub>2</sub>PSi<sub>2</sub> [M+H]<sup>+</sup> 551.3401; found 551.3397. m.p.: 123–125 °C.

#### 2,6-Bis(triisopropylsilyl)-4-phenylphospholo[2,3-c:4,5-c']dipyrrrole AuCl complex (**8-AuCl**):

A 1.6 M solution of <sup>t</sup>BuLi in <sup>n</sup>pentane (0.16 mL, 250 μmol) was added dropwise to a solution of dibromobipyrrrole **6** (30 mg, 50 μmol) in anhydrous THF (5 mL) at -78 °C under Ar atmosphere. The mixture was stirred for 10 min and then stirred for 15 min at room temperature. After recoiling to -78 °C, PhPCl<sub>2</sub> (17 μL, 125 μmol) was added by one portion. The mixture was stirred for 10 min and then warmed to room temperature. After the mixture was stirred for 60 min, AuCl(SMe<sub>2</sub>) (60 mg, 200 μmol) was added and the mixture was stirred for a further 10 min. The reaction was quenched with saturated NH<sub>4</sub>Cl aqueous solution (5 mL) and the product was extracted with CH<sub>2</sub>Cl<sub>2</sub> (10 mL ×3). The combined organic layer was washed with water and brine, and dried over Na<sub>2</sub>SO<sub>4</sub>. After the solvent was removed, the crude product was purified by silica gel chromatography using a 1:1 mixture of CH<sub>2</sub>Cl<sub>2</sub> and <sup>n</sup>hexane to give **8-AuCl** as a colorless solid (19 mg, 24 μmol, 48%). Single crystals suitable for X-ray crystallographic analysis were obtained by vapor diffusion of 2-propanol into a solution of **8-AuCl** in toluene. <sup>1</sup>H NMR (395.88 MHz, CDCl<sub>3</sub>, 25 °C): δ = 7.63 (m, 2H, *ortho*-H), 7.36 (m, 3H, *meta*-H and *para*-H), 6.90 (s, 2H, α-H), 6.81 (s, 2H, α-H), 1.44 (m, 6H, -SiCH(CH<sub>3</sub>)<sub>2</sub>) and 1.11 (dd, *J* = 10.9 Hz, *J* = 7.8 Hz, 36H, -SiCH(CH<sub>3</sub>)<sub>2</sub>) ppm; <sup>13</sup>C NMR (99.54 MHz, CDCl<sub>3</sub>, 25 °C): δ = 133.8 (d, *J* = 62 Hz), 132.8 (m), 131.2 (m), 128.8 (m), 128.1 (d, *J* = 10 Hz), 126.7 (dd, *J* = 21 Hz, *J* = 15 Hz), 123.1 (d, *J* = 85 Hz), 115.4 (dd, *J* = 14 Hz, *J* = 8.6 Hz), 17.9 (m) and 11.8 ppm; <sup>31</sup>P NMR (161.7 MHz, CDCl<sub>3</sub>, 25 °C): δ = -6.82 ppm. UV/vis (cyclohexane): λ (ε, M<sup>-1</sup> cm<sup>-1</sup>) = 267 (12000) nm. Fluorescence (cyclohexane, λ<sub>ex</sub> = 255 nm): λ<sub>max</sub> = 363 nm. FT-IR (ATR): ν = 2945, 2866, 1526, 1464, 1437, 1385, 1362, 1255, 1028, 1185, 1104, 1088, 1064, 1016, 999, 926, 883, 807, 749, 693, 667, 625, 598, 531 and 483 cm<sup>-1</sup>. HRMS (APCI, positive) calcd. for C<sub>32</sub>H<sub>52</sub>N<sub>2</sub>PSi<sub>2</sub>AuCl [M+H]<sup>+</sup> 783.2755; found 783.2742. m.p.: 209–211 °C.

#### 2,6-Bis(triisopropylsilyl)-4,4-diphenylsilolo[2,3-c:4,5-c']dipyrrrole (**9**):

A 1.6 M solution of <sup>t</sup>BuLi in <sup>n</sup>pentane (0.16 mL, 250 μmol) was added dropwise to a solution of dibromobipyrrrole **6** (30 mg, 50 μmol) in anhydrous THF (5 mL) at -78 °C under Ar atmosphere. The mixture was stirred for 10 min and then stirred for 15 min at room temperature. After recoiling to -78 °C, Ph<sub>2</sub>SiCl<sub>2</sub> (26 μL, 125 μmol) was added. The mixture was stirred for 10 min and then warmed to room temperature. After the mixture was stirred for 60 min, the reaction was quenched with water (5 mL) and the product was extracted with CH<sub>2</sub>Cl<sub>2</sub> (10 mL ×3). The combined organic layer was washed with water and brine, and dried over Na<sub>2</sub>SO<sub>4</sub>. After the solvent was removed, the crude product was purified by silica gel chromatography (Wakogel C400) using a 1:5 mixture of toluene and <sup>n</sup>hexane to give **9** as a colorless solid (13.7 mg, 22 μmol, 44%). Single crystals suitable for X-ray crystallographic analysis were

obtained by vapor diffusion of <sup>n</sup>octane into a solution of **9** in toluene. <sup>1</sup>H NMR (395.88 MHz, CDCl<sub>3</sub>, 25 °C): δ = 7.68 (m, 4H, *meta*-H), 7.32 (m, 6H, *ortho*-H and *para*-H), 6.91 (s, 2H, α-H), 6.84 (s, 2H, α-H), 1.47 (septet, *J* = 7.2 Hz, 6H, -SiCH(CH<sub>3</sub>)<sub>2</sub>) and 1.12 (d, *J* = 7.2 Hz, 36H, -SiCH(CH<sub>3</sub>)<sub>2</sub>) ppm; <sup>13</sup>C NMR (99.54 MHz, CDCl<sub>3</sub>, 25 °C): δ = 136.8, 135.6, 133.0, 129.1, 128.5, 127.7, 122.7, 115.0, 18.1 and 12.0 ppm. UV/vis (cyclohexane): λ (ε, M<sup>-1</sup> cm<sup>-1</sup>) = 261 (10000) nm. Fluorescence (cyclohexane, λ<sub>ex</sub> = 255 nm): λ<sub>max</sub> = 362 nm. FT-IR (ATR): ν = 3066, 2889, 2864, 1528, 1463, 1428, 1216, 1167, 1113, 1091, 1066, 1016, 992, 926, 882, 795, 734, 694, 664, 620, 587, 532 and 480 cm<sup>-1</sup>. HRMS (APCI, positive) calcd. for C<sub>38</sub>H<sub>57</sub>N<sub>2</sub>Si<sub>3</sub> [M+H]<sup>+</sup> 625.3824; found 625.3815. m.p.: 225–227 °C.

#### Michael-type addition of **7** with dimethyl acetylenedicarboxylate (**10**):

A solution of **7** (4.6 mg, 9.7 μmol) and dimethyl acetylenedicarboxylate (5.7 mg, 40 μmol) in toluene (0.5 mL) was stirred at 100 °C under Ar atmosphere for 12 h. After the solvent was removed, the crude product was separated by silica gel chromatography using a 1:1 mixture of CH<sub>2</sub>Cl<sub>2</sub> and <sup>n</sup>hexane to give **10** as an orange solid (1.9 mg, 3.1 μmol, 32%). <sup>1</sup>H NMR (395.88 MHz, CDCl<sub>3</sub>, 25 °C): δ = 6.99 (s, 1H), 6.80 (s, 1H), 6.62 (s, 2H), 3.71 (s, 3H, CH<sub>3</sub>), 3.45 (s, 3H, CH<sub>3</sub>), 1.44 (septet, *J* = 7.8 Hz, 3H, -SiCH(CH<sub>3</sub>)<sub>2</sub>), 1.35 (septet, *J* = 7.8 Hz, 3H, -SiCH(CH<sub>3</sub>)<sub>2</sub>), 1.14 (d, *J* = 7.8 Hz, 9H, -SiCH(CH<sub>3</sub>)<sub>2</sub>) and 1.09 (m, 27H, -SiCH(CH<sub>3</sub>)<sub>2</sub>) ppm; <sup>13</sup>C NMR (99.54 MHz, CDCl<sub>3</sub>, 25 °C): δ = 168.0, 153.7, 137.8, 130.5, 129.1, 113.3, 113.1, 53.0, 52.0, 18.5, 18.4, 18.0, 13.4 and 11.9 ppm (There is some peak overlapping). UV/vis (cyclohexane): λ (ε, M<sup>-1</sup> cm<sup>-1</sup>) = 241(sh) (18000), 263 (8300) and 441 (1800) nm. Fluorescence (cyclohexane, λ<sub>ex</sub> = 420 nm): λ<sub>max</sub> = 509 nm. FT-IR (ATR): ν = 3162, 2947, 2926, 2867, 1731, 1719, 1625, 1465, 1433, 1397, 1264, 1246, 1223, 1208, 1146, 1119, 1071, 1016, 998, 883, 796, 767, 731, 674, 656, 572 and 520 cm<sup>-1</sup>. HRMS (APCI, positive) calcd. for C<sub>32</sub>H<sub>53</sub>N<sub>2</sub>O<sub>4</sub>SSi<sub>2</sub> [M+H]<sup>+</sup> 617.3259; found 617.3250. m.p.: 145–147 °C.

## Acknowledgements

This work was supported by JSPS KAKENHI Grant Numbers 25888011 and 15K17822 (T.H.) and 25220801 (H.I.).

**Keywords:** radialene • pyrrole • charge-transfer • electron-donor • thiophene

- [1] a) H. Hopf, G. Maas, *Angew. Chem.* **1992**, *104*, 953–977; *Angew. Chem. Int. Ed. Engl.* **1992**, *31*, 931–954; b) M. Gholami, R. R. Tykwinski, *Chem. Rev.* **2006**, *106*, 4997–5027; c) G. Maas, H. Hopf in *The Chemistry of Dienes and Polyenes*, Vol. 1 (Ed.: Z. Rappoport), John Wiley and Sons, Chichester, **1997**, chapter 21, pp. 927–977.
- [2] H. Hopff, A. K. Wick, *Helv. Chim. Acta* **1961**, *44*, 19–24.
- [3] a) T. Höpfner, P. G. Jones, B. Ahrens, I. Dix, L. Ernst, H. Hopf, *Eur. J. Org. Chem.* **2003**, 2596–2611; b) S. Shinozaki, T. Hamura, Y. Ibusuki, K. Fujii, H. Uekusa, K. Suzuki, *Angew. Chem.* **2010**, *122*, 3090–3093; *Angew. Chem. Int. Ed.* **2010**, *49*, 3026–3029; c) P. J. Steel, C. J. Sumbly, *Chem. Commun.* **2002**, 322–323; d) J. D. Evans, C. A. Hollis, S. Hack, A. S. Gentleman, P. Hoffmann, M. A. Buntine, C. J. Sumbly, *J. Phys. Chem. A* **2012**, *116*, 8001–8007; e) M. Ueda, Y. Ogura, Y. Misaki, *Chem. Lett.* **2013**, *42*, 562–564; f) M. Ueda, Y. Misaki, *Org. Lett.* **2013**, *15*, 3824–3827; g) A. A. von Richthofen, L. Marzorati, L. C. Ducati, C. Di Vitto, *Org. Lett.* **2014**, *16*, 4020–4023; h) J. A. Januszewski, F. Hampel, C. Neiss, A. Görling, R. R. Tykwinski, *Angew. Chem.* **2014**, *126*, 3818–3822; *Angew. Chem. Int. Ed.* **2014**, *53*, 3743–3747.
- [4] a) A. M. Boldi, F. Diederich, *Angew. Chem.* **1994**, *106*, 482–485; *Angew. Chem. Int. Ed. Engl.* **1994**, *33*, 468–471; b) M. Schreiber, R. R. Tykwinski, F. Diederich, R. Spreiter, U. Gubler, C. Bosshard, I. Poberaj, P. Günter, C. Boudon, J.-P. Gisselbrecht, M. Gross, U. Jonas, H. Ringsdorf, *Adv. Mater.* **1997**, *9*, 339–343; c) S. Eisler, R. R. Tykwinski, *Angew. Chem.* **1999**, *111*, 2138–2141; *Angew. Chem. Int. Ed.* **1999**, *38*, 1940–1943; d) Y. Tobe, R. Umeda, N. Iwasa, M. Sonoda, *Chem. Eur. J.* **2003**, *9*, 5549–5559; e) M. Gholami, F. Melin, R. McDonald, M. J. Ferguson, L. Echegoyen, R. R. Tykwinski, *Angew. Chem.* **2007**, *119*, 9239–9243; *Angew. Chem. Int. Ed.* **2007**, *46*, 9081–9085.
- [5] a) C. Lepetit, M. B. Nielsen, F. Diederich, R. Chauvin, *Chem. Eur. J.* **2003**, *9*, 5056–5066; b) E. Konstantinova, D. S. Galvão, P. M. V. B. Barone, S. O. Dantas, *J. Mol. Struct. THEOCHEM* **2005**, *729*, 203–210; c) C. Domene, P. W. Fowler, L. W. Jenneskens, E. Steiner, *Chem. Eur. J.* **2007**, *13*, 269–276.
- [6] a) F. Wudl, R. C. Haddon, E. T. Zellers, F. B. Bramwell, *J. Org. Chem.* **1979**, *44*, 2491–2493; b) T. Sugimoto, H. Awaji, Y. Misaki, Z. Yoshida, Y. Kai, H. Nakagawa, N. Kasai, *J. Am. Chem. Soc.* **1985**, *107*, 5792–5793; c) T. Sugimoto, Y. Misaki, Y. Arai, Y. Yamamoto, Z. Yoshida, Y. Kai, N. Kasai, *J. Am. Chem. Soc.* **1988**, *110*, 628–629; d) Y. Kono, H. Miyamoto, Y. Aso, T. Otsubo, F. Ogura, T. Tanaka, M. Sawada, *Angew. Chem.* **1989**, *101*, 1254–1255; *Angew. Chem. Int. Ed. Engl.* **1989**, *28*, 1222–1224; e) T. J. LePage, R. Breslow, *J. Am. Chem. Soc.* **1987**, *109*, 6412–6421; f) M. Iyoda, H. Kurata, M. Oda, C. Okubo, K. Nishimoto, *Angew. Chem.* **1993**, *105*, 97–99; *Angew. Chem. Int. Ed. Engl.* **1993**, *32*, 89–90; g) K. Takahashi, S. Tarutani, *Adv. Mater.* **1995**, *7*, 639–641.
- [7] a) A. Patra, Y. H. Wijsboom, L. J. W. Shimon, M. Bendikov, *Angew. Chem.* **2007**, *119*, 8970–8974; *Angew. Chem. Int. Ed.* **2007**, *46*, 8814–8818; b) G. Berionni, J. I. Wu, P. v. R. Schleyer, *Org. Lett.* **2014**, *16*, 6116–6119.
- [8] a) I. Miyahara, A. Hayashi, K. Hirotsu, M. Yoshifuji, H. Yoshimura, K. Toyota, *Polyhedron* **1992**, *11*, 385–387; b) W. Brieden, T. Kellersohn, *Chem. Ber.* **1993**, *126*, 845–847; c) A. Mahieu, Y. Miquel, A. Igau, B. Donnadieu, J.-P. Majoral, *Organometallics* **1997**, *16*, 3086–3088; d) C. M. D. Komen, C. J. Horan, S. Krill, G. M. Gray, M. Lutz, A. L. Spek, A. W. Ehlers, K. Lammertsma, *J. Am. Chem. Soc.* **2000**, *122*, 12507–12516.
- [9] a) W. S. Trahanovsky, T. J. Cassidy, *J. Am. Chem. Soc.* **1984**, *106*, 8197–8201; b) F. D. Jong, M. J. Janssen, *J. Org. Chem.* **1971**, *36*, 1645–1648; c) N. Münzel, K. Kesper, A. Schweig, H. Specht, *Tetrahedron Lett.* **1988**, *29*, 6239–6242; d) C.-K. Sha, C.-P. Tsou, *Tetrahedron* **1993**, *49*, 6831–6836; e) M. Iyoda, M. Miura, S. Sasaki, S. M. H. Kabir, Y. Kuwatani, M. Yoshida, *Tetrahedron Lett.* **1997**, *38*, 4581–4582.
- [10] Expanded radialenes with heteroatom spacer are also regarded as hybrid radialenes. see a) R. R. Schumaker, S. Rajeswari, M. V. Joshi, M. P. Cava, M. A. Takassi, R. M. Metzger, *J. Am. Chem. Soc.* **1989**, *111*, 308–313; b) R. Gleiter, H. Röckel, H. Irgartinger, T. Oeser, *Angew. Chem.* **1994**, *106*, 1340–1342; *Angew. Chem. Int. Ed. Engl.* **1994**, *33*, 1270–1272; c) R. Gleiter, H. Röckel, B. Nuber, *Tetrahedron Lett.* **1994**, *35*, 8779–8782; d) T. Suzuki, T. Yoshino, J. Nishida, M. Ohkita, T. Tsuji, *J. Org. Chem.* **2000**, *65*, 5514–5521.
- [11] T. Higashino, A. Osuka, *Chem. Asian J.* **2013**, *8*, 1994–2002.
- [12] a) Crystallographic data for **7**: C<sub>26</sub>H<sub>46</sub>N<sub>2</sub>SSi<sub>2</sub>, *M<sub>r</sub>* = 474.89, monoclinic, *P*2<sub>1</sub>/*n* (No.14), *a* = 7.8062(9), *b* = 30.789(4), *c* = 11.6667(12) Å, β = 96.377(2)°, *V* = 2786.6(5) Å<sup>3</sup>, ρ<sub>calcd</sub> = 1.132 g cm<sup>-3</sup>, *Z* = 4, *R*<sub>1</sub> = 0.0378 [*I* > 2σ(*I*)], *wR*<sub>2</sub> = 0.0990 (all data), GOF = 1.031; b) Crystallographic data for **8-AuCl**: 2(C<sub>32</sub>H<sub>51</sub>AuClN<sub>2</sub>PSi<sub>2</sub>)·3(C<sub>7</sub>H<sub>8</sub>), *M<sub>r</sub>* = 1843.02, monoclinic, *P*2<sub>1</sub>/*c* (No.14), *a* = 14.5748(10), *b* = 21.3661(14), *c* = 28.275(2) Å, β = 95.5935(12)°, *V* = 8763.3(10) Å<sup>3</sup>, ρ<sub>calcd</sub> = 1.397 g cm<sup>-3</sup>, *Z* = 4, *R*<sub>1</sub> = 0.0317 [*I* > 2σ(*I*)], *wR*<sub>2</sub> = 0.0848 (all data), GOF = 1.039; c) Crystallographic data for **9**: C<sub>38</sub>H<sub>56</sub>N<sub>2</sub>Si<sub>3</sub>, *M<sub>r</sub>* = 625.11, triclinic, *P*-1 (No.2), *a* = 8.7570(9), *b* = 14.2036(17), *c* = 15.8801(16) Å, α = 76.215(3), β = 78.143(4), γ = 89.118(5)°, *V* = 1876.2(4) Å<sup>3</sup>, ρ<sub>calcd</sub> = 1.107 g cm<sup>-3</sup>, *Z* = 2, *R*<sub>1</sub> = 0.0388 [*I* > 2σ(*I*)], *wR*<sub>2</sub> = 0.1127 (all data), GOF =

- 
- 1.098; d) Crystallographic data for **10**:  $C_{32}H_{52}N_2O_4SSi_2$ ,  $M_r = 616.99$ , triclinic,  $P-1$  (No.2),  $a = 9.723(17)$ ,  $b = 12.41(2)$ ,  $c = 15.35(3)$  Å,  $\alpha = 100.55(4)$ ,  $\beta = 99.971(15)$ ,  $\gamma = 90.45(3)^\circ$ ,  $V = 1793(5)$  Å<sup>3</sup>,  $\rho_{\text{calcd}} = 1.143$  g cm<sup>-3</sup>,  $Z = 2$ ,  $R_1 = 0.0771$  [ $I > 2\sigma(I)$ ],  $wR_2 = 0.1737$  (all data), GOF = 1.025. CCDC-1061791(7), 1061792(8-AuCl), 1061793(9) and 1061794(10) contain the supplementary crystallographic data for this paper. These data can be obtained free of charge from The Cambridge Crystallographic Data Centre via [www.ccdc.cam.ac.uk/data\\_request/cif](http://www.ccdc.cam.ac.uk/data_request/cif).
- [13] K. Kveseth, R. Seip, D. A. Kohl, *Acta Chem. Scand.*, **1980**, *34A*, 31–42.
- [14] T. M. Krygowski, H. Szatyłowicz, O. A. Stasyuk, J. Dominikowska, M. Palusiak, *Chem. Rev.* **2014**, *114*, 6383–6422.
- [15] Bharat, R. Bholá, T. Bally, A. Valente, M. K. Cyrański, Ł. Dobrzycki, S. M. Spain, P. Rempala, M. R. Chin, B. T. King, *Angew. Chem.* **2010**, *122*, 409–412; *Angew. Chem. Int. Ed.* **2010**, *49*, 399–402.
- [16] a) P. v. R. Schleyer, C. Maerker, A. Dransfeld, H. Jiao, N. J. R. v. E. Hommes, *J. Am. Chem. Soc.* **1996**, *118*, 6317–6318; b) Z. Chen, C. S. Wannere, C. Cominboeuf, R. Puchta, P. v. R. Schleyer, *Chem. Rev.* **2005**, *105*, 3842–3888.
- [17] a) C. K. Lee, C. S. Hahn, W. E. Noland, *J. Org. Chem.* **1978**, *43*, 3727–3729; b) W. E. Noland, C. K. Lee, *J. Org. Chem.* **1980**, *45*, 4573–4582.
- [18] J. Pommerehne, H. Vestweber, W. Guss, R. F. Mahrt, H. Bässler, M. Porsch, J. Daub, *Adv. Mater.* **1995**, *7*, 551–554.
- [19] a) T. Kadoya, M. Ashizawa, T. Higashino, T. Kawamoto, S. Kumeta, H. Matsumoto, T. Mori, *Phys. Chem. Chem. Phys.* **2013**, *15*, 17818–17822; b) K. Seki, *Mol. Cryst. Liq. Cryst.* **1989**, *171*, 255–270.
- [20] a) K. P. Goetz, D. Vermeulen, M. E. Payne, C. Kloc, L. E. McNeil, O. D. Jurchescu, *J. Mater. Chem. C* **2014**, *2*, 3065–3076; b) H. Akamatu, H. Inokuchi, Y. Matsunaga, *Bull. Chem. Soc. Jpn.* **1956**, *29*, 213–218; c) J. Ferraris, D. O. Cowan, V. Walatka, Jr., J. H. Perlstein, *J. Am. Chem. Soc.* **1973**, *95*, 948–949.
- [21] a) M. A. M. Leenen, F. Cucinotta, L. Viani, A. Mavrinskiy, W. Pisula, J. Gierschner, J. Cornil, A. Prodi-Schwab, H. Thiem, K. Müllen, L. De Cola, *J. Phys. Chem. B* **2010**, *114*, 14614–14620; b) H. Jung, H. Hwang, K.-M. Park, J. Kim, D.-H. Kim, Y. Kang, *Organometallics* **2010**, *29*, 2715–2723.
- [22] a) S. Yamaguchi, K. Tamao, *Chem. Lett.* **2005**, *34*, 2–7; b) X. Zhan, S. Barlow, S. R. Marder, *Chem. Commun.* **2009**, 1948–1955.
-

---

## Entry for the Table of Contents (Please choose one layout)

Layout 2:

### FULL PAPER

---



*T. Higashino, H. Imahori\**

**Hybrid [5]Radialenes with  
Bispyrroloheteroles: New Electron-  
Donating Units**

From the X-ray crystal structures and calculated natural bond orbital (NBO) bond orders, bispyrroloheteroles were found to be as the rare examples of structurally characterized hybrid [5]radialenes. They are promising as novel electron-donating building blocks for charge-transporting and donor/acceptor photovoltaic materials.

---

## Contents

1. High-Resolution MS
2. NMR Spectra
3. X-Ray Crystallographic Details
4. Optical Properties
5. DFT Calculations
6. References

# 1. High-Resolution MS

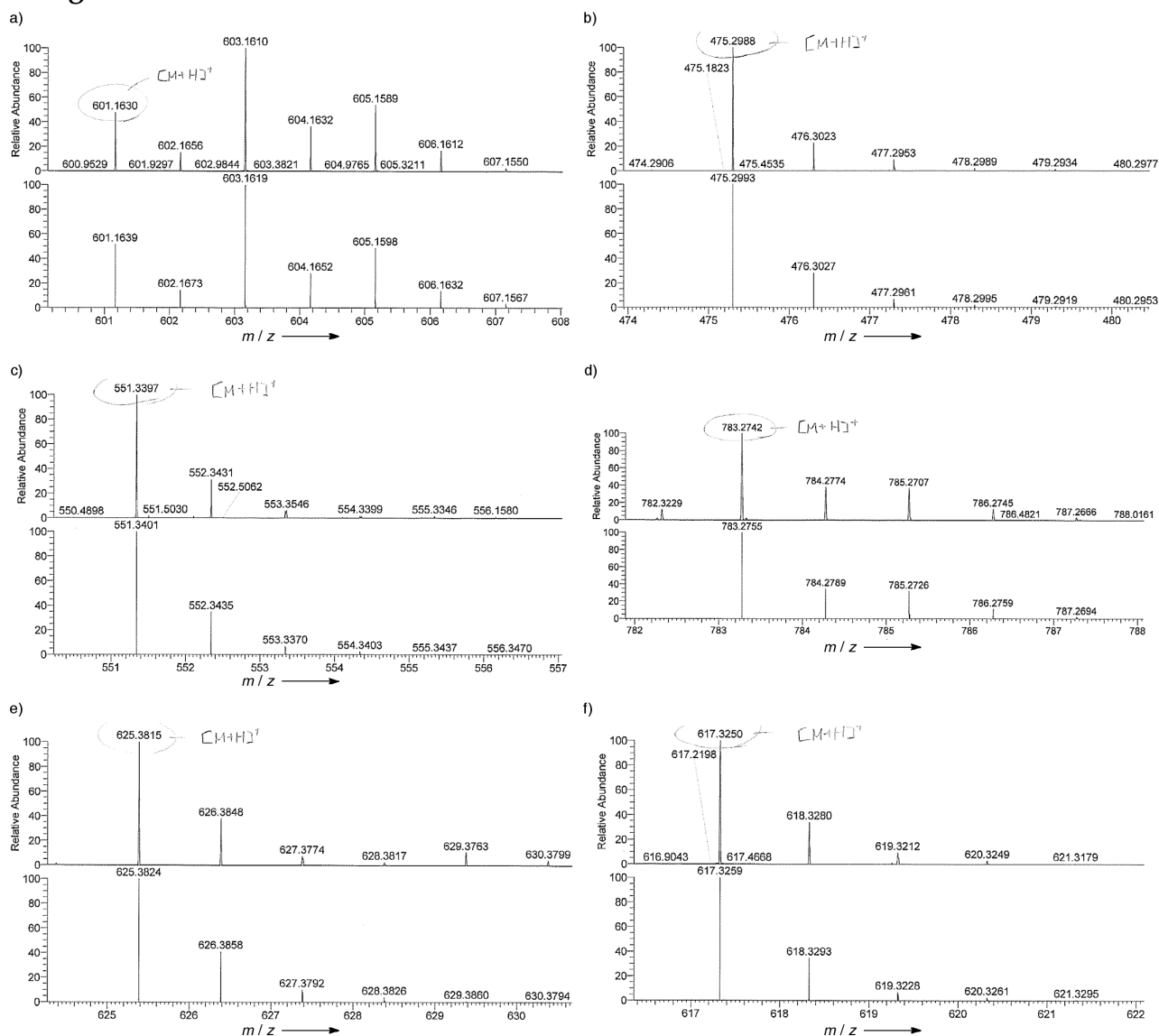


Figure S1. Observed (top) and simulated (bottom) high-resolution APCI-MS of a) 6, b) 7, c) 8, d) 8-AuCl, e) 9, and f) 10.

## 2. NMR Spectra

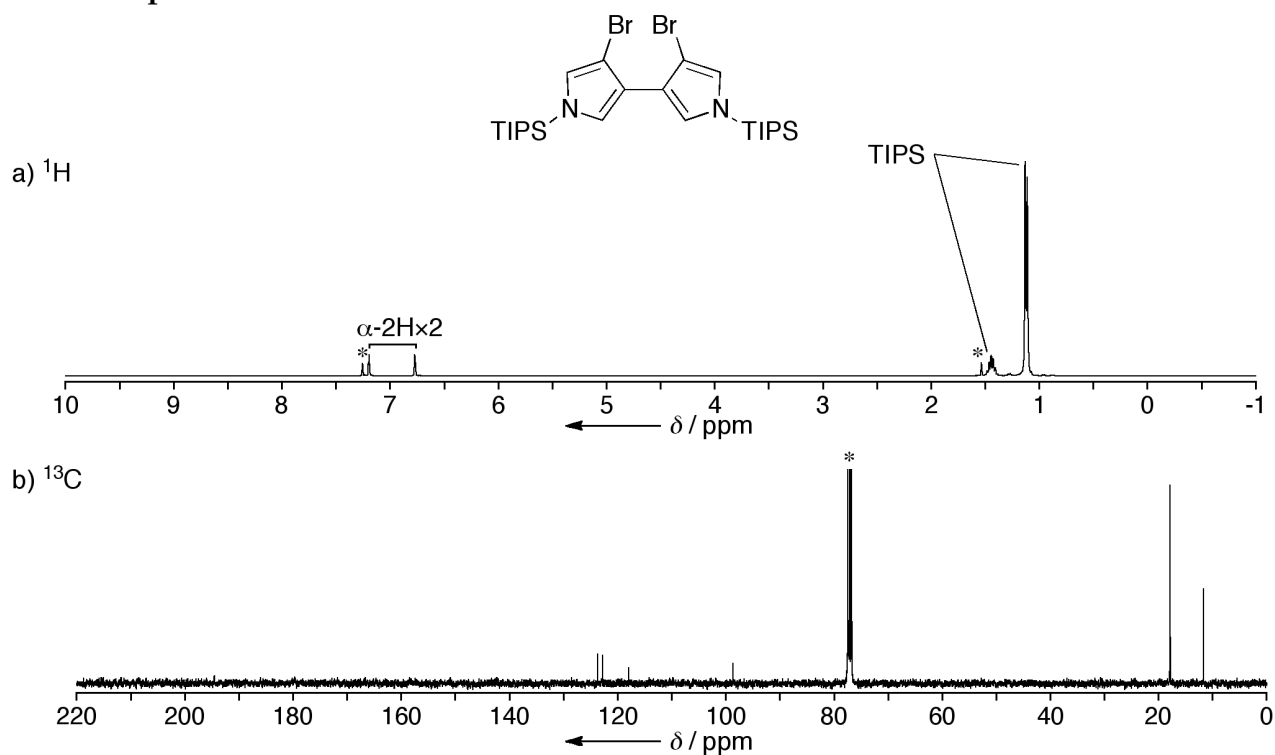


Figure S2. a)  $^1\text{H}$  and b)  $^{13}\text{C}$  NMR spectra of 6 at 25 °C in  $\text{CDCl}_3$ . Peaks marked with \* are due to residual solvents.

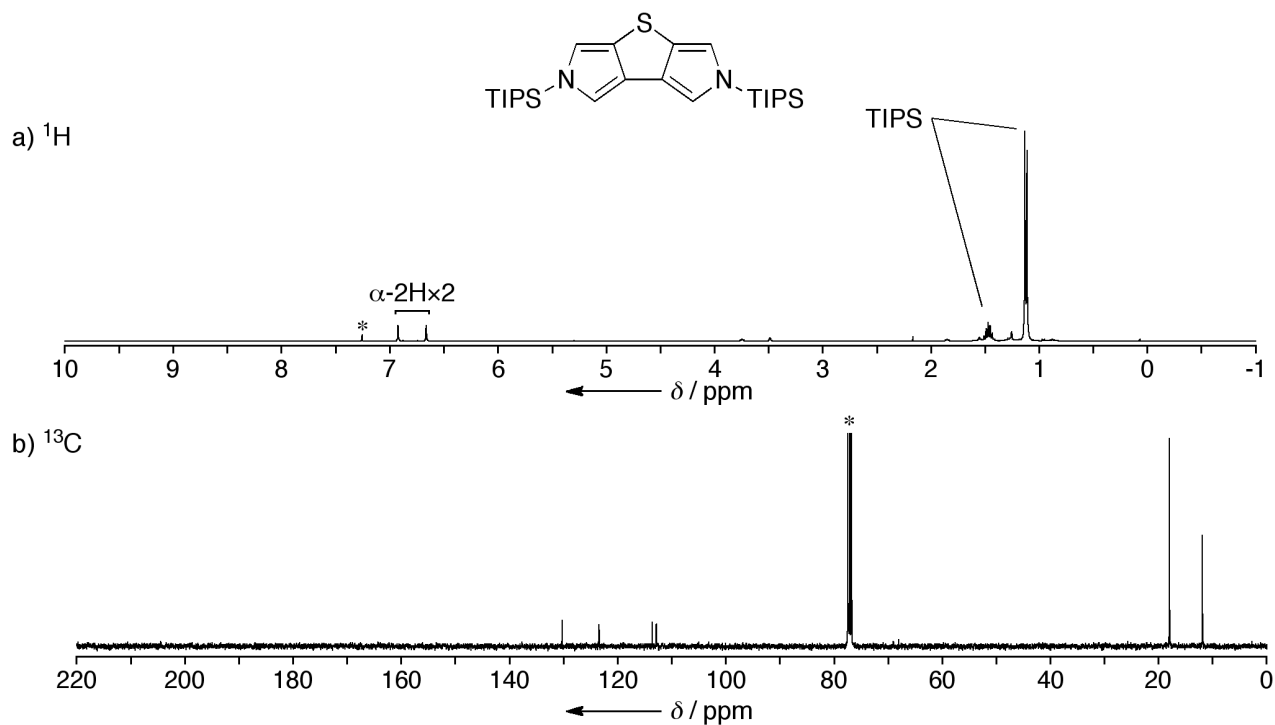
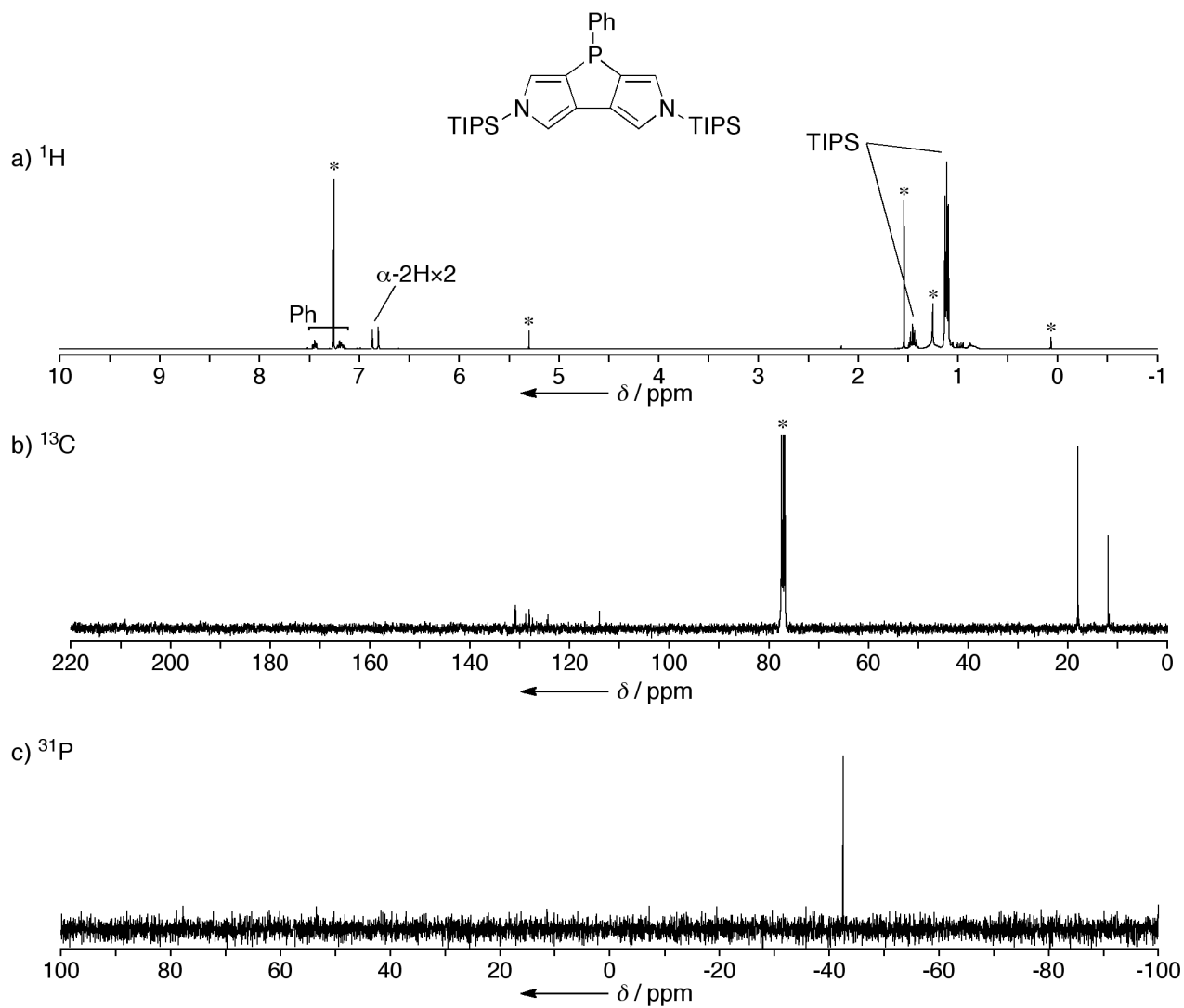
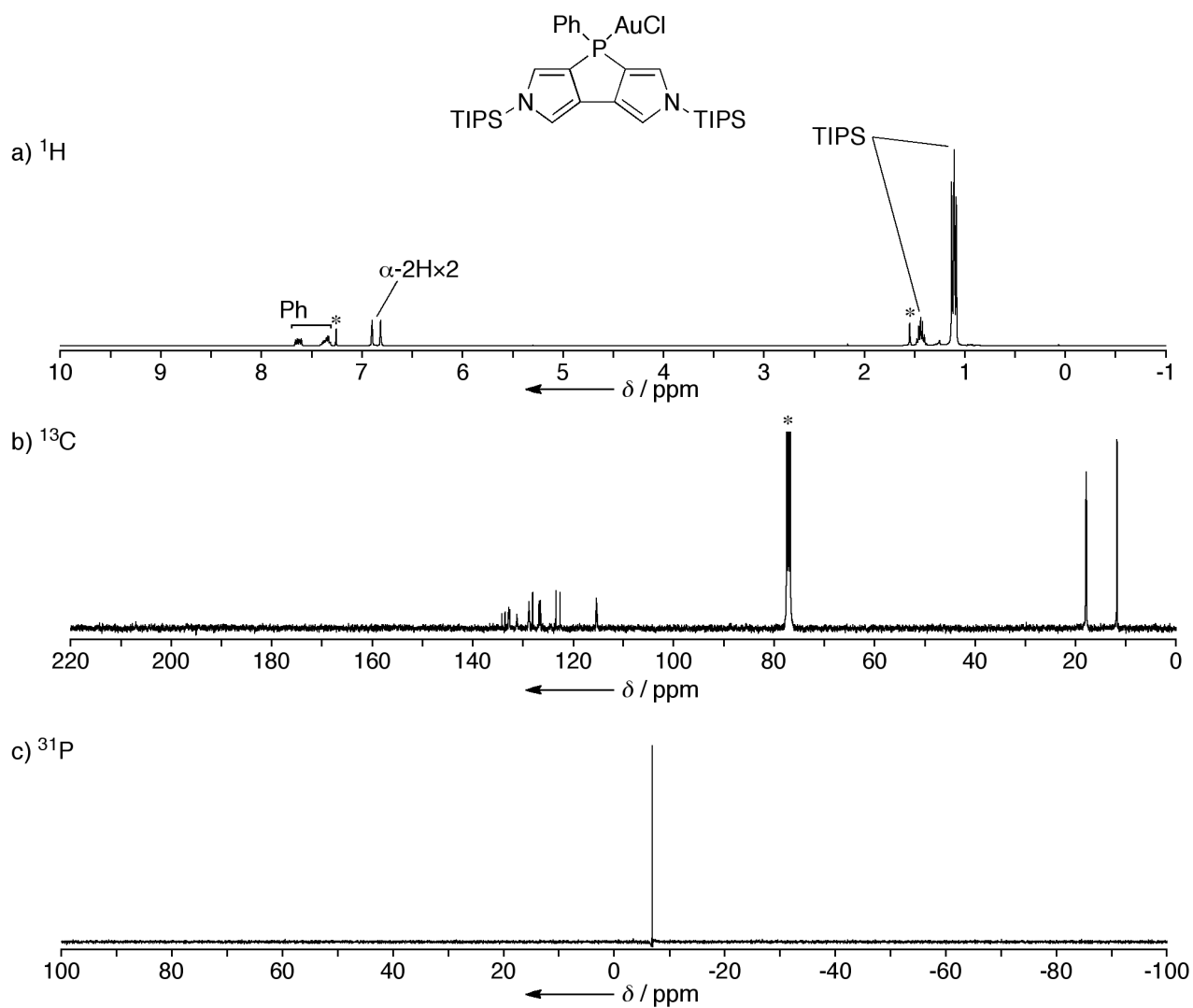


Figure S3. a)  $^1\text{H}$  and b)  $^{13}\text{C}$  NMR spectra of 7 at 25 °C in  $\text{CDCl}_3$ . Peaks marked with \* are due to residual solvents.



**Figure S4.** a)  $^1\text{H}$ , b)  $^{13}\text{C}$ , and c)  $^{31}\text{P}$  NMR spectra of **8** at 25 °C in  $\text{CDCl}_3$ . Peaks marked with \* are due to residual solvents.



**Figure S5.** a)  $^1\text{H}$ , b)  $^{13}\text{C}$ , and c)  $^{31}\text{P}$  NMR spectra of **8-AuCl** at 25 °C in  $\text{CDCl}_3$ . Peaks marked with \* are due to residual solvents.

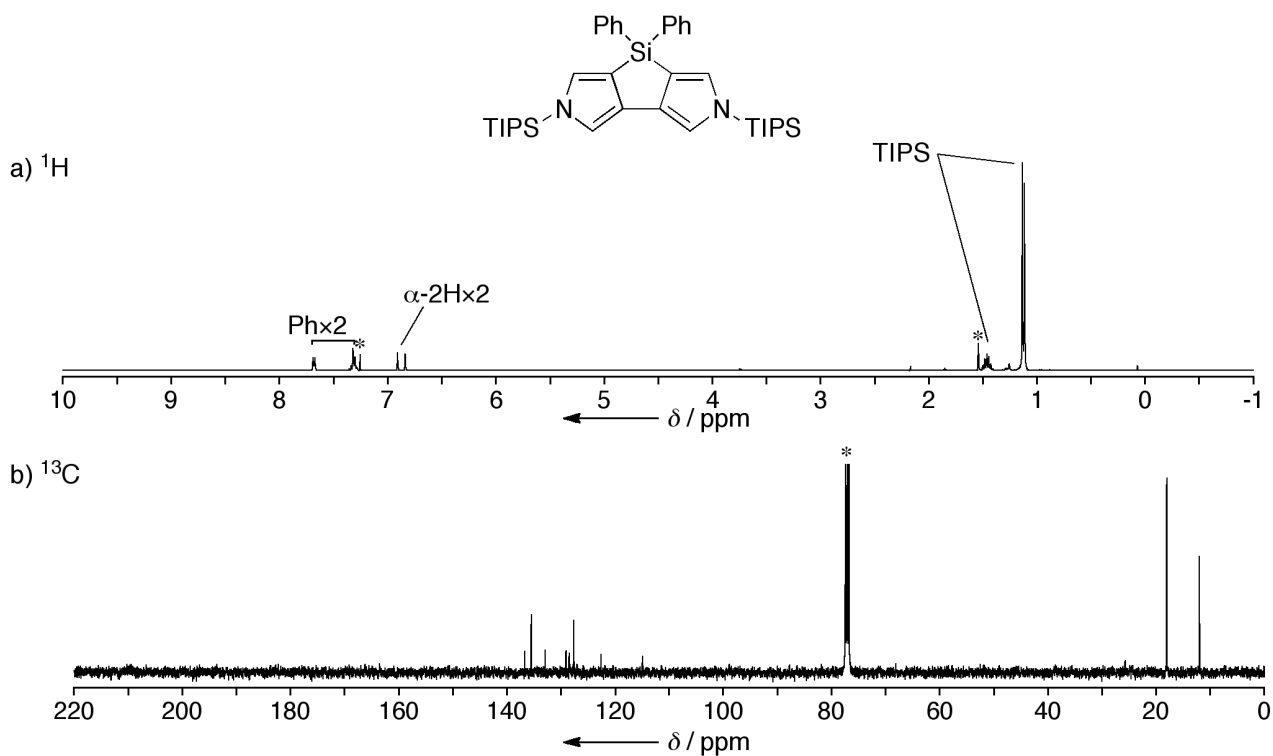


**Figure S6.** a)  $^1\text{H}$  and b)  $^{13}\text{C}$  NMR spectra of **9** at 25 °C in  $\text{CDCl}_3$ . Peaks marked with \* are due to residual solvents.

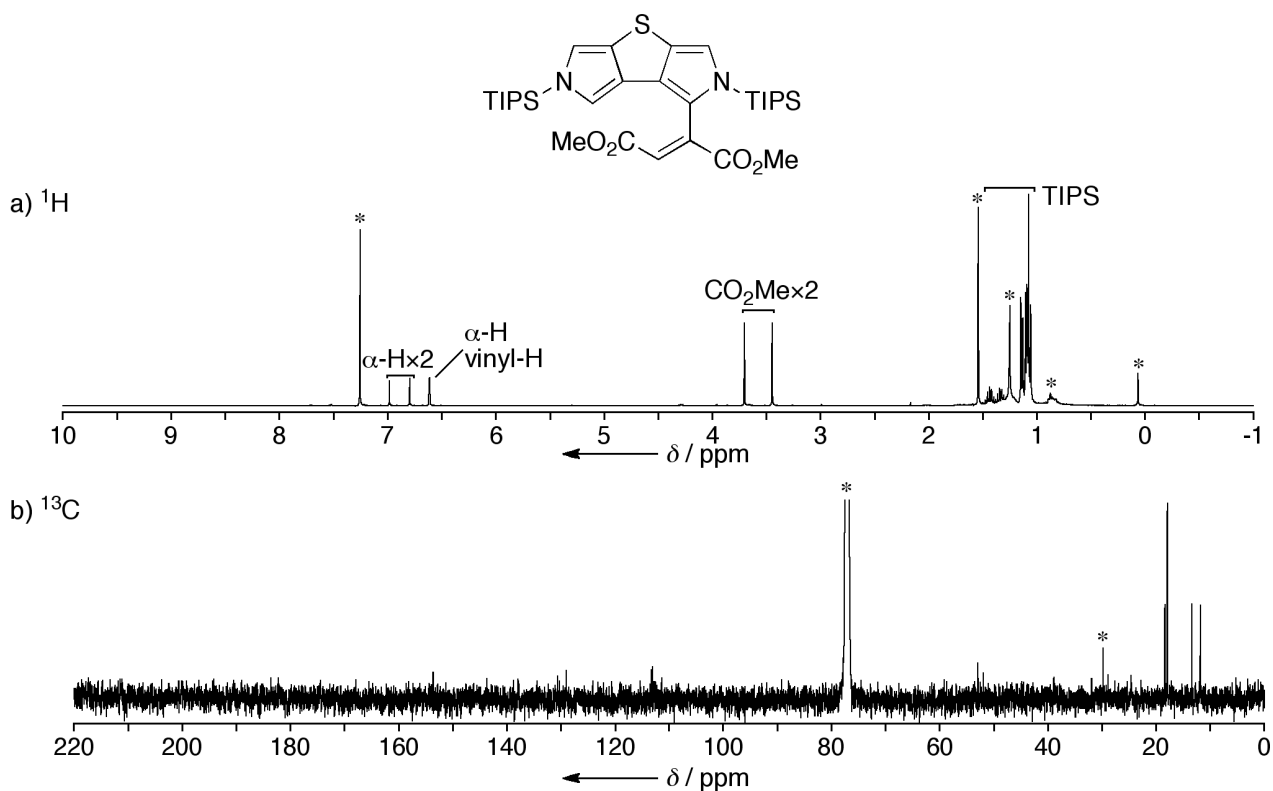


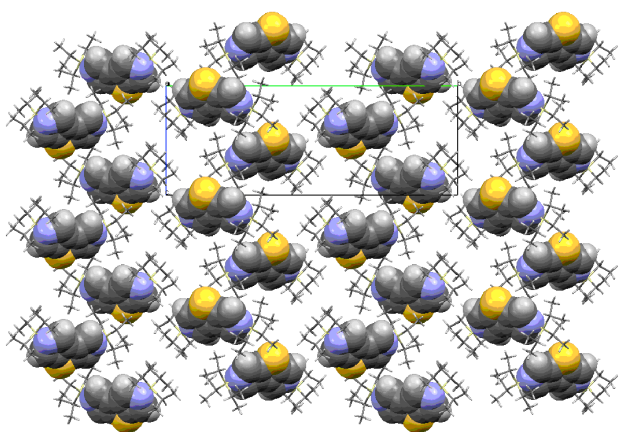
**Figure S7.** a)  $^1\text{H}$  and b)  $^{13}\text{C}$  NMR spectra of **10** at 25 °C in  $\text{CDCl}_3$ . Peaks marked with \* are due to residual solvents.

### 3. X-Ray Crystallographic Details

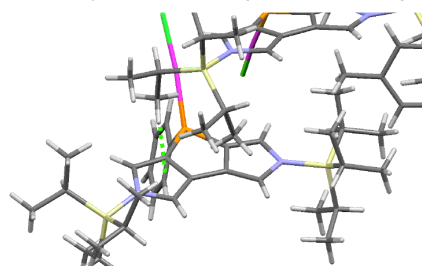
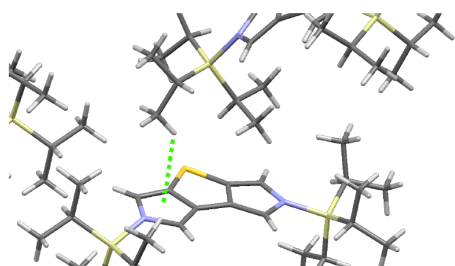
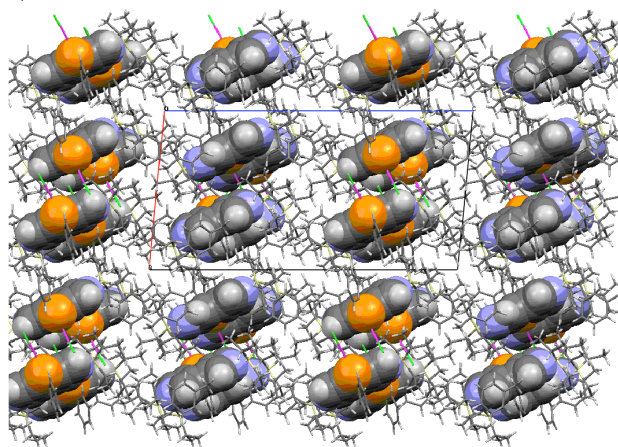
**Table S1.** Crystal data of **7**, **8-AuCl**, **9**, and **10**.

	<b>7</b>	<b>8-AuCl</b>	<b>9</b>	<b>10</b>
formula	C <sub>26</sub> H <sub>46</sub> N <sub>2</sub> SSi <sub>2</sub>	2(C <sub>32</sub> H <sub>51</sub> AuClN <sub>2</sub> PSi <sub>2</sub> )· 3(C <sub>7</sub> H <sub>8</sub> )	C <sub>38</sub> H <sub>56</sub> N <sub>2</sub> Si <sub>3</sub>	C <sub>32</sub> H <sub>52</sub> N <sub>2</sub> O <sub>4</sub> SSi <sub>2</sub>
<i>M</i> <sub>r</sub>	474.89	1843.02	625.11	616.99
<i>T</i> [K]	123(2)	123(2)	123(2)	123(2)
crystal system	monoclinic	monoclinic	triclinic	triclinic
space group	<i>P</i> 2 <sub>1</sub> / <i>n</i> (No.14)	<i>P</i> 2 <sub>1</sub> / <i>c</i> (No.14)	<i>P</i> -1 (No.2)	<i>P</i> -1 (No.2)
<i>a</i> [Å]	7.8062(9)	14.5748(10)	8.7570(9)	9.723(17)
<i>b</i> [Å]	30.789(4)	21.3661(14)	14.2036(17)	12.41(2)
<i>c</i> [Å]	11.6667(12)	28.275(2)	15.8801(16)	15.35(3)
$\alpha$ [°]	90	90	76.215(3)	100.55(4)
$\beta$ [°]	96.377(2)	95.5935(12)	78.143(4)	99.971(15)
$\gamma$ [°]	90	90	89.118(5)	90.45(3)
<i>V</i> [Å <sup>3</sup> ]	2786.6(5)	8763.3(10)	1876.2(4)	1793(5)
<i>Z</i>	4	4	2	2
$\rho_{\text{calcd}}$ [g cm <sup>-3</sup> ]	1.132	1.397	1.107	1.143
<i>F</i> [000]	1040	3768	680	668
crystal size [mm <sup>3</sup> ]	0.50×0.10×0.10	0.40×0.20×0.20	0.50×0.30×0.10	0.50×0.10×0.10
2 $\theta_{\text{max}}$ [°]	54.98	54.96	54.98	54.42
reflections collected	22404	70842	15222	12833
independent reflections	6194	20021	8215	7456
parameters	292	919	400	384
<i>R</i> <sub>1</sub> [ <i>I</i> > 2 $\sigma$ ( <i>I</i> )]	0.0378	0.0317	0.0338	0.0771
<i>wR</i> <sub>2</sub> [all data]	0.1052	0.0848	0.1127	0.1737
GOF	1.031	1.039	1.098	1.025
CCDC number	1061791	1061792	1061793	1061794

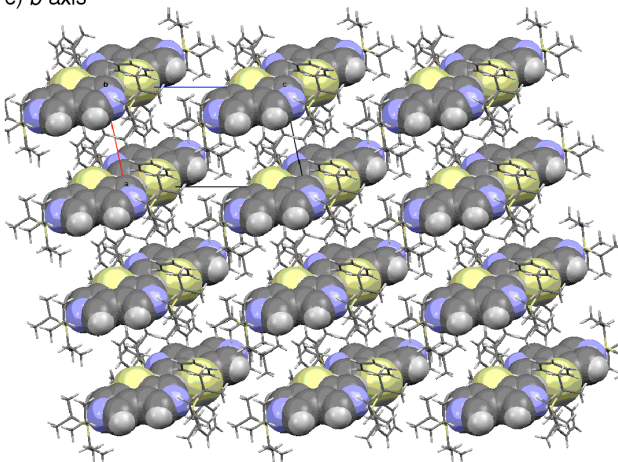
a) *a*-axis



b) *b*-axis



c) *b*-axis



d) *c*-axis

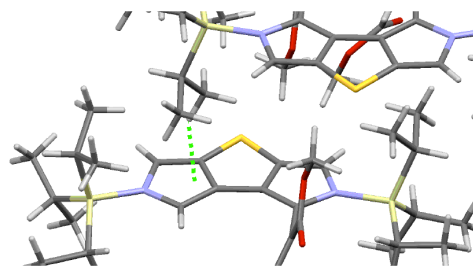
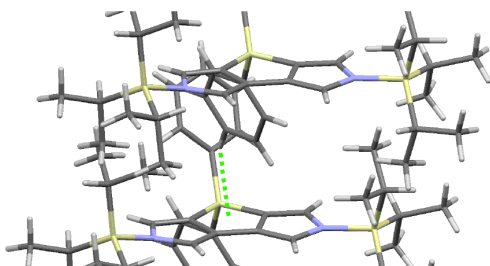
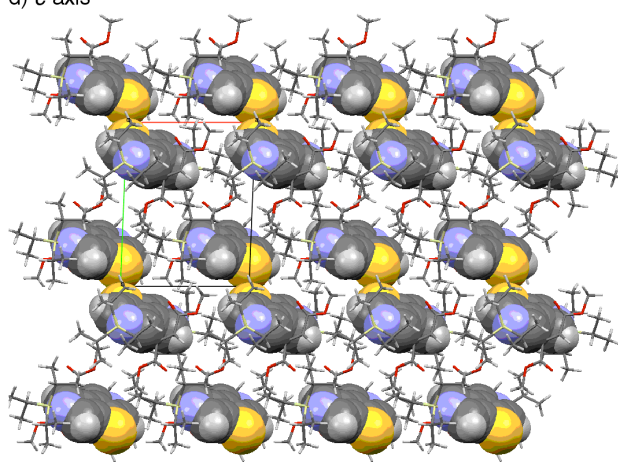


**Figure S8.** Packing structures of a) 7, b) 8-AuCl, c) 9, and d) 10. Intermolecular CH... $\pi$  interactions are also shown as green dotted lines.

## 4. Optical Properties

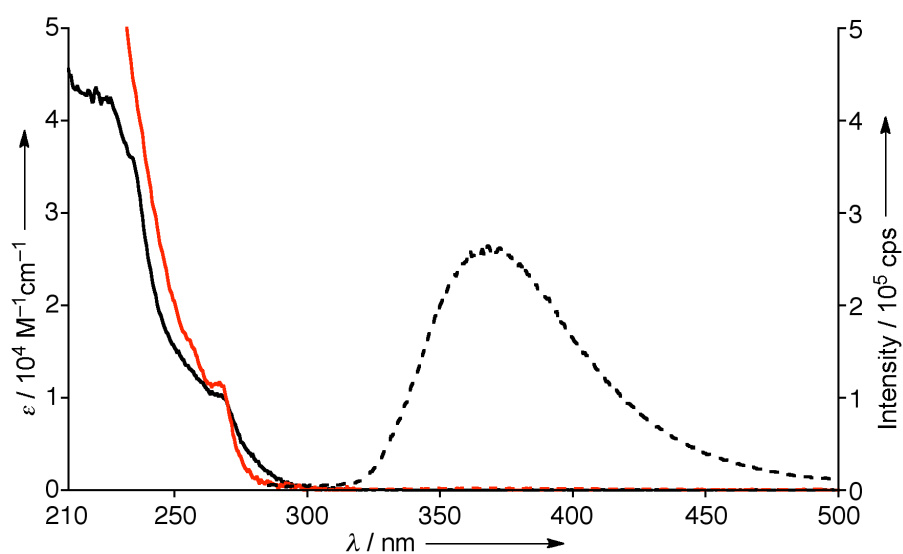


**Figure S9.** UV/Vis absorption (solid line) and fluorescence spectra (dashed line) of **8** (black) and **8-AuCl** (red) in cyclohexane. For the fluorescence measurements, the absorbances at 255 nm were adjusted to be identical (0.1) and the samples were excited at 255 nm under the same excitation condition for accurate intensity comparison.

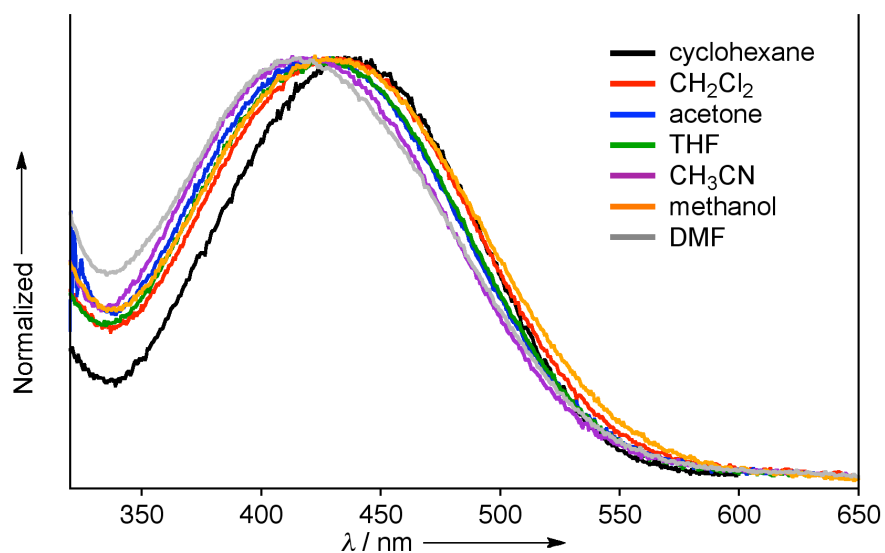


**Figure S10.** UV/Vis absorption spectra of **10** in various solvents. Compound **10** reveals negative solvatochromism, which is similar to that of TTF-based D- $\pi$ -A molecules.<sup>[S1,S2]</sup>

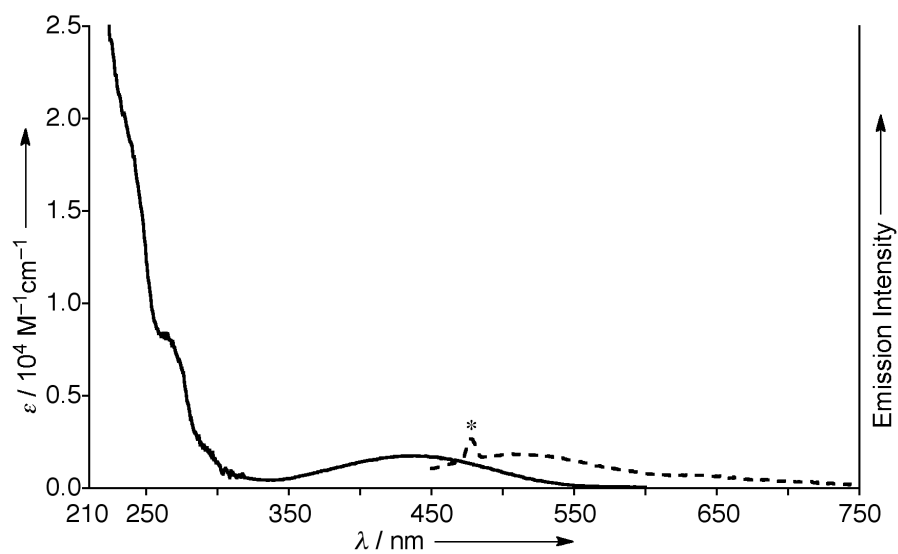


**Figure S11.** UV/Vis absorption (solid line) and fluorescence spectra (dashed line) of **10** in cyclohexane. Sample was excited at 420 nm. Peak marked with \* is due to excitation light.

## 5. DFT Calculations

All calculations were carried out using the *Gaussian 09* program.<sup>[S3]</sup> All structures were fully optimized without any symmetry restriction. The calculations were performed by the density functional theory (DFT) method with restricted B3LYP (Becke's three-parameter hybrid exchange functionals and the Lee-Yang-Parr correlation functional) level,<sup>[S4,S5]</sup> employing a basis set 6-31G(d,p) for C, H, O, N, Si, P, and S. The NICS values were obtained with the GIAO method at the B3LYP/6-31G(d,p) level. Excitation energies and oscillator strengths for the optimized structures were calculated with the TD-SCF method at the B3LYP/6-31G(d,p) level.

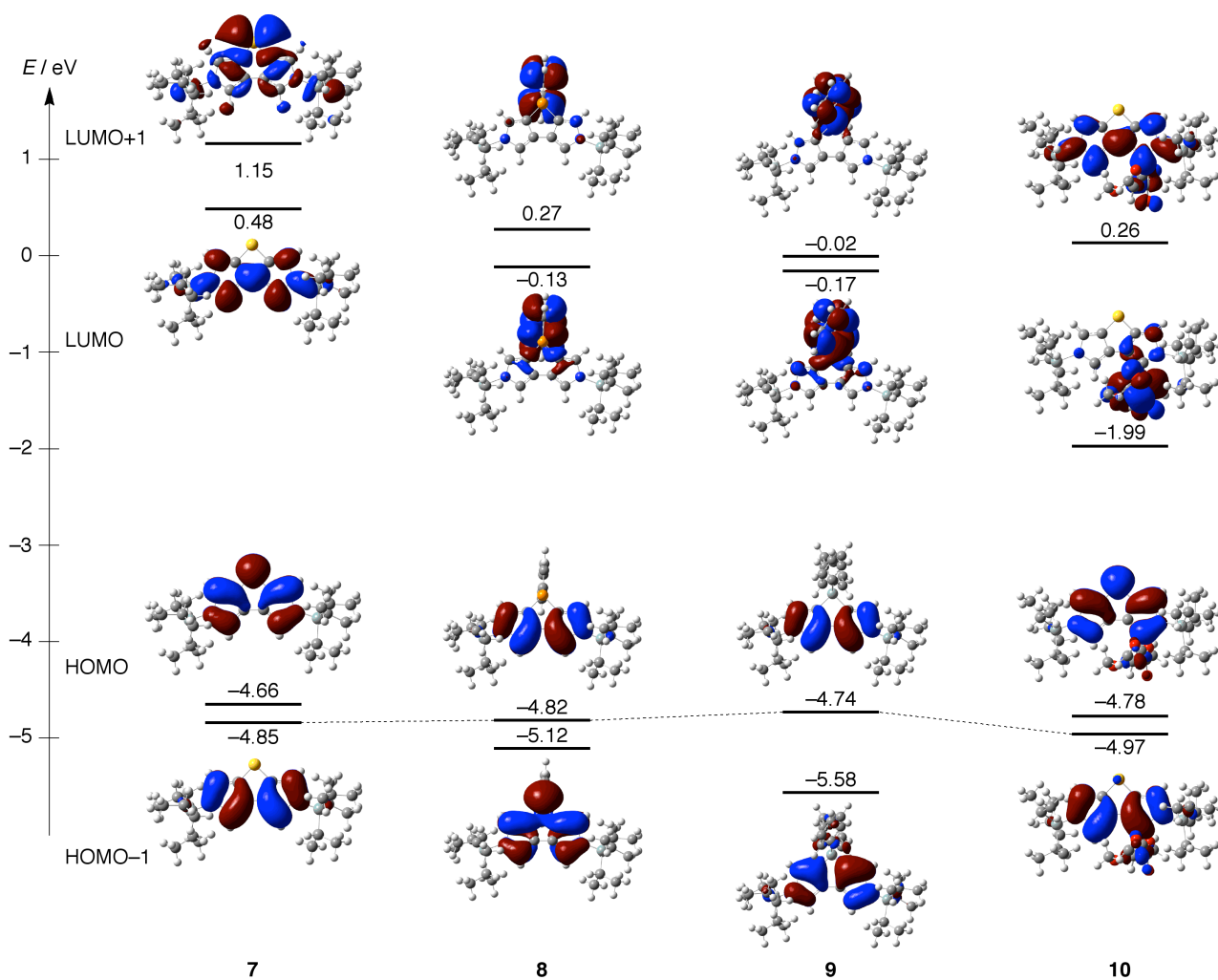


Figure S12. Selected Kohn-Sham orbitals of bispyrroloheteroles 7–10.

**Table S2.** Selected excitation energies and oscillator strengths of **7–10** calculated by the TD-DFT method.

state	excitation energy		oscillator	excitation			weight [%]
	[eV]	[nm]	strength				
<b>7</b>							
1	4.56	272	0.0085	HOMO	→	LUMO	68
				HOMO-1	→	LUMO+2	13
3	5.06	245	0.4422	HOMO-1	→	LUMO	68
				HOMO-2	→	LUMO	11
5	5.36	231	0.3051	HOMO	→	LUMO+2	64
				HOMO-1	→	LUMO	14
<hr/>							
<b>8</b>							
1	4.08	304	0.0004	HOMO	→	LUMO	70
5	4.73	262	0.0252	HOMO	→	LUMO+2	55
				HOMO	→	LUMO+3	39
6	4.84	256	0.0250	HOMO-2	→	LUMO	70
8	5.10	243	0.3366	HOMO	→	LUMO+3	51
<hr/>							
<b>9</b>							
1	4.00	310	0.0018	HOMO	→	LUMO	70
6	4.81	258	0.0324	HOMO-2	→	LUMO	70
7	4.84	256	0.0312	HOMO	→	LUMO+4	60
10	5.15	241	0.2679	HOMO	→	LUMO+5	48
				HOMO	→	LUMO+4	31
<hr/>							
<b>10</b>							
1	2.20	564	0.0288	HOMO	→	LUMO	62
7	4.46	278	0.0110	HOMO	→	LUMO+1	63
				HOMO-4	→	LUMO	16
11	4.83	256	0.2495	HOMO-1	→	LUMO+1	64
				HOMO-1	→	LUMO+2	15

## 6. References

- [S1] R. Andreu, I. Malfant, P. G. Lacroix, P. Cassoux, *European J. Org. Chem.* **2000**, 737–741.
- [S2] M. R. Bryce, A. Green, A. J. Moore, D. F. Perepichka, A. S. Batsanov, J. A. K. Howard, I. Ledoux-Rak, M. González, N. Martín, J. L. Segura, J. Garín, J. Orduna, R. Alcalá, B. Villacampa, *European J. Org. Chem.* **2001**, 1927–1935.
- [S3] Gaussian 09, Revision D.01, M. J. Frisch, G. W. Trucks, H. B. Schlegel, G. E. Scuseria, M. A. Robb, J. R. Cheeseman, G. Scalmani, V. Barone, B. Mennucci, G. A. Petersson, H. Nakatsuji, M. Caricato, X. Li, H. P. Hratchian, A. F. Izmaylov, J. Bloino, G. Zheng, J. L. Sonnenberg, M. Hada, M. Ehara, K. Toyota, R. Fukuda, J. Hasegawa, M. Ishida, T. Nakajima, Y. Honda, O. Kitao, H. Nakai, T. Vreven, J. A. Montgomery, Jr., J. E. Peralta, F. Ogliaro, M. Bearpark, J. J. Heyd, E. Brothers, K. N. Kudin, V. N. Staroverov, T. Keith, R. Kobayashi, J. Normand, K. Raghavachari, A. Rendell, J. C. Burant, S. S. Iyengar, J. Tomasi, M. Cossi, N. Rega, J. M. Millam, M. Klene, J. E. Knox, J. B. Cross, V. Bakken, C. Adamo, J. Jaramillo, R. Gomperts, R. E. Stratmann, O. Yazyev, A. J. Austin, R. Cammi, C. Pomelli, J. W. Ochterski, R. L. Martin, K. Morokuma, V. G. Zakrzewski, G. A. Voth, P. Salvador, J. J. Dannenberg, S. Dapprich, A. D. Daniels, O. Farkas, J. B. Foresman, J. V. Ortiz, J. Cioslowski, D. J. Fox, Gaussian, Inc., Wallingford CT, **2013**.
- [S4] A. D. Becke, *J. Chem. Phys.* **1993**, 98, 1372–1377.
- [S5] C. Lee, W. Yang, R. G. Parr, *Phys. Rev. B*, **1998**, 37, 785–789.